

**MICROWAVE-ASSISTED SYNTHESIS AND
ELECTROCHEMICAL STUDIES OF 5-ETHOXYCARBONYL-
6-METHYL-4-(*p*-TOLYL)-3,4-DIHYDROPYRIMIDIN-2(1*H*)-
ONE**

GOH WEE SHENG

**BACHELOR OF SCIENCE (HONS)
CHEMISTRY**

**FACULTY OF SCIENCE
UNIVERSITI TUNKU ABDUL RAHMAN
MAY 2014**

**MICROWAVE-ASSISTED SYNTHESIS AND
ELECTROCHEMICAL STUDIES OF 5-ETHOXYCARBONYL-
6-METHYL-4-(*p*-TOLYL)-3,4-DIHYDROPYRIMIDIN-2(1*H*)-
ONE**

By

GOH WEE SHENG

A project report submitted to the Department of Chemical Science
Faculty of Science
Universiti Tunku Abdul Rahman
in partial fulfillment of the requirements for the degree of
Bachelor of Science (Hons) Chemistry

May 2014

ABSTRACT

MICROWAVE-ASSISTED SYNTHESIS AND ELECTROCHEMICAL STUDIES OF 5-ETHOXYCARBONYL-6-METHYL-4-(*p*-TOLYL)-3,4-DIHYDROPYRIMIDIN-2(1*H*)-ONE

The title compound, 5-ethoxycarbonyl-6-methyl-4-(*p*-tolyl)-3,4-dihydropyrimidin-2(1*H*)-one, was synthesized via a microwave assisted solvent free three component one pot reaction involving 4-methylbenzaldehyde, ethyl acetoacetate, and urea in 83% yield. Cyclic voltammetry of the 3,4-dihydropyrimidin-2(1*H*)-one in various solvent systems showed an anodic peak at the region of 1.41 V to 1.56 V which would be enhanced and facilitated by the addition of potassium hydroxide suggesting the involvement of proton ejection in the reaction. Controlled potential electrolysis of the 3,4-dihydropyrimidin-2(1*H*)-one in solvent composition 80% acetonitrile with 20% methanol gave **GWS002** in 17% yield. Exchange of solvent composition to 50% acetonitrile with 50% methanol gave **GWS003** in 12% yield, while the reaction in solvent composition 50% acetonitrile with 50% acetone gave **GWS004** in 19% yield. The electrolysis was carried out in a three-electrode electrochemical cell equipped with a porous cylindrical carbon cage working electrode, non-isolated platinum coil wire counter electrode, and silver-silver chloride reference electrode. The products were characterized by spectroscopic methods, such as ¹H NMR, ¹³C NMR, 2D NMR, and IR. The results showed that the solvents could react with the intermediate resulted from the electrode process. This discovery provides a useful

tool in developing and modifying pyrimidinone compounds and their derivatives which are important in pharmaceutical and therapeutic usages.

ABSTRAK

SINTESIS BERBANTU GELOMBANG MIKRO DAN KAJIAN ELEKTROKIMIA 5-ETOKSIKARBONIL -6-METIL-4-(*p*-TOLIL)-3,4-DIHIDROPIRIMIDIN-2(1*H*)-ON

Sebatian, 5-etoksikarbonil-6-metil-4-(*p*-tolil)-3,4-dihidropirimidin-2(1*H*)-on, telah disintesis melalui tindak balas tanpa pelarut bantuan gelombang mikro dalam satu reaksi yang melibatkan 4-metilbenzaldehyd, etil asetoasetat dan urea dengan kajian hasil 83%. Kajian kitaran voltametri bagi 3,4-dihidropirimidin-2(1*H*)-on dalam pelbagai sistem pelarut memaparkan puncak anodik di sekitar 1.41 V kepada 1.56 V yang boleh dipermudahkan dengan penambahan kalium hidroksida yang mencadangkan penglibatan kehilangan proton dalam tindak balas. Kawalan potensi elektrolisis 3,4-dihidropirimidin-2(1*H*)-on di dalam campuran pelarut asetonitril 80% kepada pelarut dengan metanol 20% memberi **GWS002** dalam hasil 17%, sementara perubahan komposisi pelarut asetonitril 50% dengan 50% metanol memberi **GWS003** dalam hasil 12%, dan dalam komposisi pelarut 50% asetonitril pelarut dengan aseton 50% memberi **GWS004** dalam hasil sebanyak 19%, masing-masing. Kajian elektrolisis telah dijalankan dalam sisten sel elektrokimia tiga-elektrod yang dilengkapi dengan elektrod sangkar karbon porus, elektrod gegelung platinum dawai tanpa terasing (elektrod berlawanan) dan elektrod rujukan klorida argentum-argentum. Hasil-hasil tulen yang diasingkan telah dikenal pasti dengan kaedah analisis spektroskopik ¹H NMR, ¹³C NMR, 2D NMR dan IR. Hasil kajian menunjukkan bahawa pelarut mungkin bertindak balas

dengan sebatuan pirimidon. Penemuan ini menyediakan alat yang berguna dalam semasa elektrolisis dan ini membolehkan perubahan berlaku bagi terbitan pirimidon yang berkemungkinan berguna dalam farmaseutikal dan pengubatan penyakit.

ACKNOWLEDGEMENTS

This research is not my individual achievement instead is the results of help and support from many people all of this while. Firstly, I would like to express my sincere gratitude and appreciation to my supervisor, Associate Professor Dr. Lim Tuck Meng for his encouraging and giving me invaluable advice throughout the period of completion on this project. He is also willing to sacrifice his precious time to provide teaching and guidance which I valued greatly.

Other than that, I would like to thank my university, Universiti Tunku Abdul Rahman (UTAR), for the good environment and also facilities to complete this project. Also, I am obliged to all the laboratory officers in UTAR for their cooperation and help throughout the project.

Moreover, I am thankful to my course mates as well as seniors for providing support, guidance and encouragement. I am grateful that they are willing to lend me a helping hand when the need arises although everyone is as busy as I am. Last but not least, an honourable mention goes to my family and also friends for their understanding, support and constant encouragement in completing the project.

DECLARATION

I hereby declare that the project report is based on my original work except for quotations and citations which have been duly acknowledged. I also declare that it has not been previously or concurrently submitted for any other degree at UTAR or other institutions.

(GOH WEE SHENG)

APPROVAL SHEET

This project report entitled "MICROWAVE-ASSISTED SYNTHESIS AND ELECTROCHEMICAL STUDIES OF 5-ETHOXYCARBONYL-6-METHYL-4-(*p*-TOLYL)-3,4-DIHYDROPYRIMIDIN-2(1*H*)-ONE" was prepared by GOH WEE SHENG and submitted as partial fulfillment of the requirements for the degree of Bachelor of Science (Hons) Chemistry at Universiti Tunku Abdul Rahman.

Approved by:

(Assoc. Prof. Dr. LIM TUCK MENG)

Date:.....

Supervisor

Department of Chemical Science

Faculty of Science

Universiti Tunku Abdul Rahman

FACULTY OF SCIENCE
UNIVERSITI TUNKU ABDUL RAHMAN

Date: _____

PERMISSION SHEET

It is hereby certified that **GOH WEE SHENG** (ID No: **11ADB01894**) has completed this final year project entitled “MICROWAVE-ASSISTED SYNTHESIS AND ELECTROCHEMICAL STUDIES OF 5-ETHOXYCARBONYL-6-METHYL-4-(*p*-TOLYL)-3,4-DIHYDROPYRIMIDIN-2(1*H*)-ONE” supervised by Assoc. Prof. Dr. LIM TUCK MENG from the Department of Chemical Science, Faculty of Science.

I hereby give permission to my supervisor to write and prepare manuscripts of these research findings for publishing in any form, if I do not prepare it within six (6) months from this data, provided that my name is included as one of the authors for this article. The arrangement of the name depends on my supervisor.

Yours truly,

(GOH WEE SHENG)

TABLE OF CONTENTS

	Page
ABSTRACT	ii
ACKNOWLEDGEMENTS	vi
DECLARATION	vii
APPROVAL SHEET	viii
PERMISSION SHEET	ix
TABLE OF CONTENTS	x
LIST OF TABLES	xiv
LIST OF FIGURES	xv
LIST OF ABBREVIATIONS	xvii

CHAPTER

1	INTRODUCTION	1
1.1	Organic Electrochemistry	1
1.2	Electrode-Solution Interface	2
1.3	Electro-Organic Reactions	3
	1.3.1 Anodic Oxidation	4
	1.3.2 Cathodic Reduction	5
1.4	Experimental Parameters in Electro-Organic Reactions	7
	1.4.1 Solvent-Supporting Electrolyte	7
	1.4.2 The Substrate	8
	1.4.3 The Electrode Material	9
	1.4.4 The Temperature	9
1.5	Techniques for the Study of Electro-Organic Reactions	10
	1.5.1 Cyclic Voltammetry	10
	1.5.2 Controlled Potential Electrolysis	11

	1.5.3	Coulometry	12
1.6		Components of Electrochemical Cell	12
	1.6.1	Working Electrode	14
	1.6.2	Counter Electrode	14
	1.6.3	Reference Electrode	15
	1.6.4	Electrolyte Solution	15
	1.6.5	Separators and Membranes	16
1.7		Microwave-Assisted Synthesis	17
1.8		Biginelli Reaction	18
1.9		Objectives of Study	19
2		LITERATURE REVIEW	20
	2.1	Electrochemical Studies of Heterocyclic Amines	20
		2.1.1 Pyridines	20
		2.1.2 Pyrimidines	22
		2.1.3 Pyrimidinones	26
	2.2	Microwave-Assisted Synthesis of 3,4-Dihydropyrimidin-2(1 <i>H</i>)-ones	29
3		MATERIALS AND METHODS	31
	3.1	Chemicals	31
	3.2	Instrumentation	32
	3.3	Experimental Procedure	32
		3.3.1 Microwave-Assisted Synthesis of 5-Ethoxycarbonyl-6-methyl-4-(<i>p</i> -tolyl)-3,4-dihydropyrimidin-2(1 <i>H</i>)-one	32
		3.3.2 Electrochemical Studies of 5-Ethoxycarbonyl-6-methyl-4-(<i>p</i> -tolyl)-3,4-dihydropyrimidin-2(1 <i>H</i>)-one	33
		3.3.2.1 Cyclic Voltammetry	33
		3.3.2.2 Controlled Potential Electrolysis	34

	3.3.2.3	Isolation and Purification	35
	3.3.3	Characterization	36
	3.3.3.1	Nuclear Magnetic Resonance (NMR) Spectroscopy	36
	3.3.3.2	High Resolution Electrospray Ionization Quadrupole-Time of Flight (HRESIQ-TOF) Liquid Chromatography Mass Spectrometry	36
	3.3.3.3	Fourier Transform Infrared (FTIR) Spectroscopy	37
4		RESULTS AND DISCUSSION	38
	4.1	Microwave-Assisted Synthesis of 5-Ethoxycarbonyl-6-methyl-4-(<i>p</i> -tolyl)-3,4-dihydropyrimidin-2(<i>1H</i>)-one	38
	4.2	Electrochemical Studies of 5-Ethoxycarbonyl-6-methyl-4-(<i>p</i> -tolyl)-3,4-dihydropyrimidin-2(<i>1H</i>)-one	49
	4.2.1	Electrolysis of 5-Ethoxycarbonyl-6-methyl-4-(<i>p</i> -tolyl)-3,4-dihydropyrimidin-2(<i>1H</i>)-one in 80% Acetonitrile-Methanol	51
	4.2.2	Electrolysis of 5-Ethoxycarbonyl-6-methyl-4-(<i>p</i> -tolyl)-3,4-dihydropyrimidin-2(<i>1H</i>)-one in 50% Acetonitrile-Methanol	65
	4.2.3	Electrolysis of 5-Ethoxycarbonyl-6-methyl-4-(<i>p</i> -tolyl)-3,4-dihydropyrimidin-2(<i>1H</i>)-one in 50% Acetonitrile-Acetone	76
5		CONCLUSION AND FURTHER STUDIES	85
		REFERENCES	86

LIST OF TABLES

Table		Page
3.1	List of chemicals	31
3.2	List of instruments	32
4.1	Physical appearance, melting point, and R_f of GWS001	38
4.2	Molecular formula and its respective molecular ion as well as double and equivalent of GWS001 provided by HRESIMS.	39
4.3	FTIR spectrum interpretation of GWS001	40
4.4	NMR spectra interpretation of GWS001	46
4.5	Summary for the results of electrochemical studies	50
4.6	Molecular formula and its respective molecular ion as well as double and equivalent of GWS002 provided by HRESIMS.	54
4.7	FTIR spectrum interpretation of GWS002	55
4.8	NMR spectra interpretation of GWS002	61
4.9	Molecular formula and its respective molecular ion as well as double and equivalent of GWS003 provided by HRESIMS	66
4.10	FTIR spectrum interpretation of GWS003	67
4.11	NMR spectra interpretation of GWS003	73
4.12	FTIR spectrum interpretation of GWS004	77
4.13	NMR spectra interpretation of GWS004	82

LIST OF FIGURES

Figure		Page
1.1	Representation of electrode-solution interface	2
1.2	Electrode oxidation as combination of electrode process and chemical process	4
1.3	Cyclic voltammogram of reversible (curve X) and irreversible (curve Y) oxidation	11
1.4	Typical setup of an electrochemical cell	13
4.1	MS spectrum of GWS001	41
4.2	FTIR spectrum of GWS001 (thin film on KBr glass)	42
4.3	Structure of GWS001	43
4.4	^1H NMR spectrum of GWS001 in CDCl_3 (400 MHz)	47
4.5	^{13}C NMR spectrum of GWS001 in CDCl_3 (100 MHz)	48
4.6	Cyclic voltammogram of GWS001 (5 mg) at glassy carbon rod working electrode, isolated platinum wire counter electrode, and silver-silver chloride reference electrode in 80% acetonitrile-methanol.	52
4.7	MS spectrum of GWS002	56
4.8	FTIR spectrum of GWS002 (thin film on KBr glass)	57
4.9	Proposed structure of GWS002	58
4.10	Selected HMBC correlations	60
4.11	^1H NMR spectrum of GWS002 in CDCl_3 (400 MHz)	62
4.12	^{13}C NMR spectrum of GWS002 in CDCl_3 (100 MHz)	63

4.13	Cyclic voltammogram of GWS001 (5 mg) at glassy carbon rod working electrode, isolated platinum wire counter electrode, and silver-silver chloride reference electrode in 50% acetonitrile-methanol.	65
4.14	MS spectrum of GWS003	68
4.15	FTIR spectrum of GWS003 (thin film on KBr glass)	69
4.16	Proposed structure of GWS003	70
4.17	Selected HMBC correlations	72
4.18	^1H NMR spectrum of GWS003 in CDCl_3 (400 MHz)	74
4.19	^{13}C NMR spectrum of GWS003 in CDCl_3 (100 MHz)	75
4.20	Cyclic voltammogram of GWS001 (5 mg) at glassy carbon rod working electrode, isolated platinum wire counter electrode, and silver-silver chloride reference electrode in 50% acetonitrile-acetone.	76
4.21	FTIR spectrum of GWS004 (thin film on KBr glass)	78
4.22	Proposed structure of GWS004	79
4.23	Selected HMBC correlations	81
4.24	^1H NMR spectrum of GWS04 in CDCl_3 (400 MHz)	83
4.25	^{13}C NMR spectrum of GWS004 in CDCl_3 (100 MHz)	84

LIST OF ABBREVIATIONS

δ	Chemical shift
J	Coupling constant
CDCl_3	Deuterated chloroform
DHPs	Dihydropyrimidinones
DEPT	Distortionless Enhancement by Polarization Transfer
d	Doublet
FTIR	Fourier Transform Infrared
HMBC	Heteronuclear Multiple Bond Correlation
HRESIQ-TOF	High Resolution Electrospray Ionization Quadrupole-Time of Flight
HRESIQ-TOFLC/MS	High Resolution Electrospray Ionization Quadrupole-Time of Flight Liquid Chromatography Mass Spectrometer
HRESIMS	High Resolution Electrospray Ionization Mass Spectrometry
KBr	Potassium bromide
MS	Mass Spectrometry
NMR	Nuclear Magnetic Resonance
NOESY	Nuclear Overhauser Effect Spectroscopy
q	Quartet
R_f	Retardation factor
s	Singlet
t	Triplet

CHAPTER 1

INTRODUCTION

1.1 Organic Electrochemistry

Organic electrochemistry is the study on the oxidation and reduction of organic molecules at electrodes. It is studied by using electrochemical cells. Electrochemical cells basically consist of electrodes and electrolyte solution. The electrode has the ability to supply and accept electrons, which can be exactly adjusted by changing of the electrode potential. Electrolyte solution is a substance that contains free ions and has the ability to conduct electricity.

The two important effects, which are mass transfer and current transport through the solution, results from the property that electrode provides and receives electrons to and from molecules. Mass transfer is the transfer of molecules from the homogeneous bulk solution to the heterogeneous surface. This causes a spatial structuring in the nearness of the electrode surface, which provides benefit to control the chemical pathway followed by an intermediate. Current transport provides the advantage of an exact alteration of the driving force through the electrode potential. (Lund and Hammerich, 2001)

1.2 Electrode-Solution Interface

The electrode-solution interface is a discontinuous plane corresponding to the electrical charge distribution. It consists of electrode, double layer, diffusion layer, and the bulk of the solution. The double layer is formed by the adsorption of ions and neutral molecules on the electrode surface with thickness of 10 \AA . The diffusion layer is the area between the double layer and the bulk of the solution. It is formed by an uneven distribution of charge with thickness of $50\text{-}100 \text{ \AA}$. In fact, the ions of opposite charge with respect to the electrode are attracted towards the electrode, but the ions having the same charge with the electrode are repelled away from the electrode. This electrostatic interaction is reduced as the distance from the electrode surface increases, resulting in the formation of double layer, diffusion layer, and bulk of the solution.

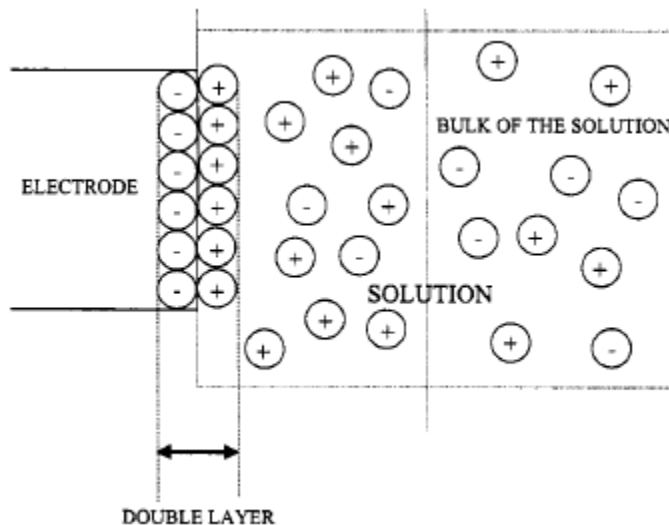
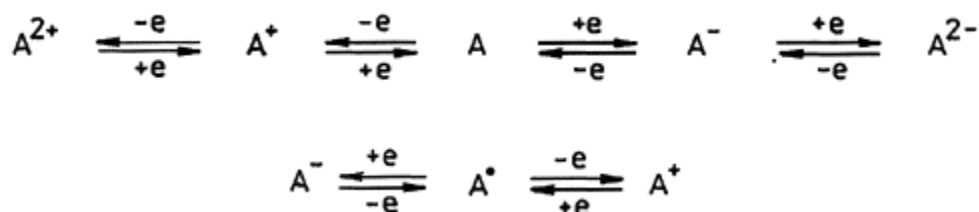


Figure 1.1: Representation of electrode-solution interface. (Zanello, 2003. p. 11)

1.3 Electro-Organic Reactions

The two processes, which are the electrode process and the chemical process, comprise an electro-organic reaction. A heterogeneous electron transfer between the electrode and the substrate without subsequent reaction is known as the electrode process. This results in the formation of an intermediate, such as a radical ion or radical. The formation of the intermediate is based on the electron configuration of the substrate and either oxidation or reduction takes place. Oxidation is the reaction that involves the removal of electrons from a substrate. Reduction reaction is the additional of electrons to a substrate.



Scheme 1.1: Possible electrode processes. (Volke and Liška, 1994. p. 4)

The chemical processes, such as addition, substitution, elimination, and rearrangement, constitute the further reactions of the intermediate formed in the electrode process. This process is controlled by the choice of solvent-supporting electrolyte, electrode material, temperature, and so on. The heterogeneous electron transfer takes place through outer-sphere mechanism (Maskill, 2006). The heterogeneous electron transfer occurs when the substrate molecule is situated very close to the double layer. In outer-sphere mechanism, electron is

transferred between the electrode and the substrate through the ions and solvent molecules adsorbed on the electrode surface (Zanello, 2003). Once the intermediate is formed, it moves away from the electrode surface and may go through chemical reactions in the diffusion layer or the bulk of solution.

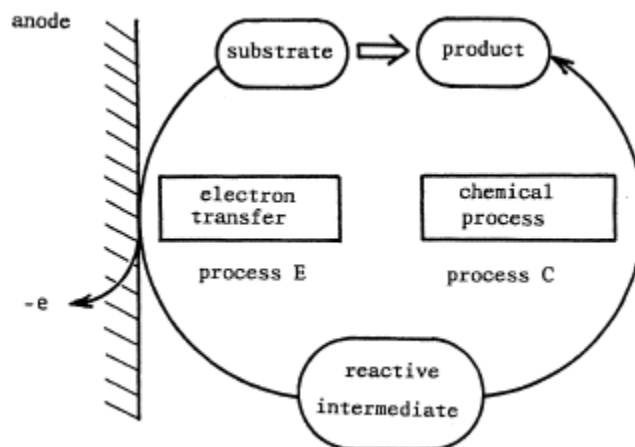
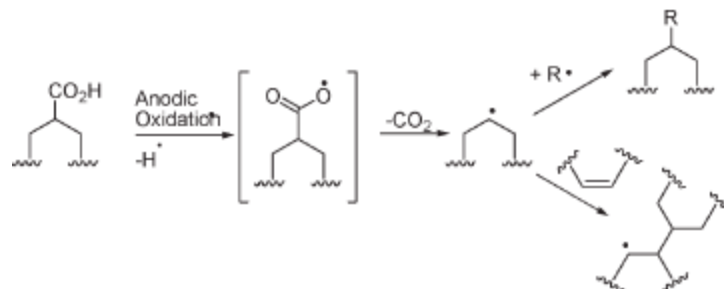


Figure 1.2: Electrode oxidation as combination of electrode process and chemical process. (Volke and Liška, 1994. p. 4)

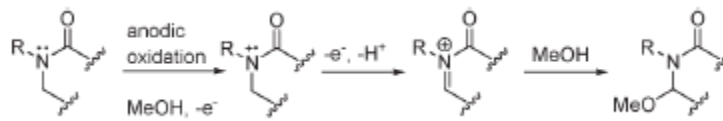
1.3.1 Anodic Oxidation

Anodic oxidation is the removal of electron from substrate on the anode electrode. The two popular anodic oxidations are Kolbe electrolysis reaction (Scheme 1.2) and Shono oxidation (Scheme 1.3). The Kolbe electrolysis reaction produces a carbon-centered radical from the electrochemical decarboxylation of a carboxylic acid. This radical can go through dimerization or addition to alkene. It can also enable radical chain reactions.



Scheme 1.2: The Kolbe electrolysis reaction producing carbon-centered radicals. (Sperry and Wright, 2006. p. 608)

The Shono oxidation is the oxidation of amides to produce an *N*-acyliminium ion. This protocol is useful in synthesizing natural products and asymmetric building blocks for organic synthesis. In addition to that, this method is applicable in medicinal chemistry.

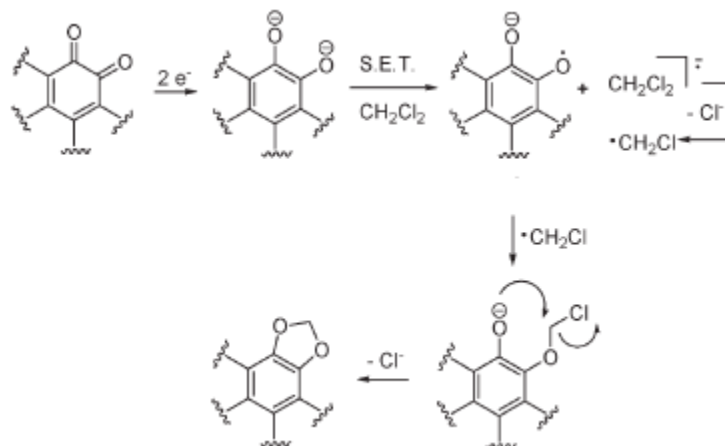


Scheme 1.3: The Shono oxidation forming *N*-acyliminium ions. (Sperry and Wright, 2006. p. 608)

1.3.2 Cathodic Reduction

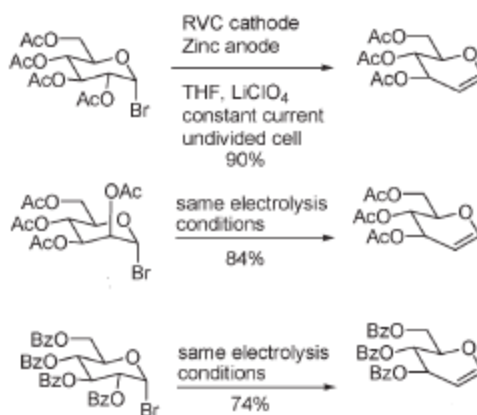
Cathodic reduction is the addition of electron to a substrate on the cathode electrode. For example, the electrochemical reduction of *o*-quinones in dichloromethane generates 1,2-dioxolanes (Scheme 1.4). First, a dianion is formed by the cathodic reduction of *o*-quinone. In solution, one-electron transfer from the dianion to dichloromethane results in the formation of

monochloromethane radical by the cleavage of one C—Cl bond. The new C—O bond is formed by the coupling of the monochloromethane radical with the quinone radical anion. 1,3-dioxolane is formed by an intramolecular nucleophilic substitution.



Scheme 1.4: Mechanism for the generation of 1,2-dioxolanes from *o*-quinones. (Sperry and Wright, 2006. p. 611)

The reported cathodic reduction of glycosyl bromides provides an alternative way to synthesize glycals (Scheme 1.5). Glycals are useful synthons and in the synthesis of *C*-glycoside and oligosaccharide. As compared to the standard methods for the synthesis of glycals, metallic or organometallic reagents are not involved in this protocol. Another example of cathodic reduction is the electrochemical reduction of aliphatic carboxylic esters or amides to primary alcohol or amines. The reduction of esters or amides generally involves four-electron transfer. The cathodic reduction of esters or amides is considered to be very hard because of their relatively high reduction potentials (~ -3.0 V versus SCE).



Scheme 1.5: Cathodic reduction of glycosyl bromides. (Sperry and Wright, 2006. p. 612)

1.4 Experimental Parameters in Electro-Organic Reactions

1.4.1 Solvent-Supporting Electrolyte

Solvent-supporting electrolyte plays an important role for the electrode process since it functions as a medium for the electro-organic reaction. Solvent itself may serve as a source of nucleophiles in the chemical process. The two criteria for a good solvent-supporting electrolyte are that it must possess high conductivity for the current and it must have good solvent properties for substrate. The conductivity is affected by the dielectric constant of solvent and the concentration of supporting electrolyte. The dielectric constant is the ability of a solvent to insulate positive charge ions from negative charge ions dissolved in that solvent. The solvent should possess a high dielectric constant in order to minimize the interaction between positive and negative charge ions. This interaction will cause a decrease in the conductivity of electric current. The concentration of supporting

electrolyte must be rather high in order to have a good conductivity for the current, and hence the concentration should not be less than 0.1 M (Eberson and Schäfer, 1971).

In non-aqueous solvent-supporting electrolyte, the anodic and cathodic limit or the accessible potential range of a solvent-supporting electrolyte is greatly dependent on the electrochemical property of the solvent or supporting electrolyte. For instance, the anodic limit in dimethyl sulfoxide is because of oxidation of solvent and the cathodic limit is due to the reduction of cation. In aqueous solvent-supporting electrolyte, the anodic and cathodic limit is reliant on the redox reaction of water. The redox potentials are different for different electrode materials.

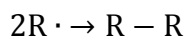
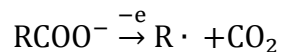
1.4.2 The Substrate

The substrate must be able to be oxidized or reduced within the given potential range which is decided by the solvent-supporting electrolyte system. Besides that, the cathodic and anodic limits of the solvent-supporting electrolyte have to be beyond the range in which the substrate reacts in order to avoid the solvent-supporting electrolyte being oxidized or reduced. Otherwise the electrolysis will not give products producing only from the electrochemical reaction of the substrate. If there is no nucleophile or electrophile exists in the solution, the

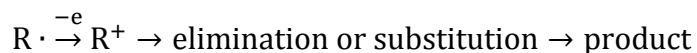
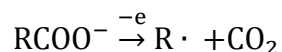
intermediate formed in the electrode process may undergo polymerization, resulting in the formation of a film on the electrode.

1.4.3 The Electrode Material

The electrode material plays an important role in determining the product of an electrochemical reaction. In cathodic reduction, the yield of the desired product highly depends on the cathode material. In the Kolbe electrolysis reaction, a platinum anode is normally used to obtain the desired yield of product formed by radical pathway.



However, products resulted from the carbonium ion pathway (two-electron transfer) are formed desirably if carbon anodes are used.



1.4.4 The Temperature

The diffusion rate of a substrate to the electrode increases as the temperature is increased. As a result, a higher current is allowed to pass through the electrolyte. Since the organic electrode process normally takes place at a very small current densities (around 10 mA/cm²), an increase in cell temperature has the advantage

of shortening electrolysis time. (Ebersson and Schäfer, 1971) However, this is impracticable when volatile materials are used. This is because volatile materials are very difficult to be retained in the cell at higher temperatures.

1.5 Techniques for the Study of Electro-Organic Reactions

1.5.1 Cyclic Voltammetry

Cyclic voltammetry is a very popular voltammetric technique due to its short analysis time and ease of interoperation. In this technique, the potential is changed in a cyclic pattern by an increase in potential with time in either direction, followed by the scan in the opposite direction and a decrease in potential with time at the same potential scan rate (Ebersson and Schäfer, 1971). The resulting cyclic voltammogram consists of a curve of current (in A) versus potential (in V). There are three parameters, which include the potential limits as well as the direction of the initial scan, the scan rate, and the number of cycles recorded, can be controlled in the cyclic voltammetric studies. Cyclic voltammetry is useful in identifying the redox potential of the substrate and understanding the intermediates formed in electrode process. In a cyclic voltammogram, when the peak appears in the positive scan direction it indicates an oxidation but when the peak appears in the negative scan direction it indicates a reduction. Generally, irreversible and reversible curves will be observed in most of the cases. In contrast, symmetrical redox potential peaks will be observed in reversible curve.

In some cases, quasireversible curve will be observed. Intermediate studies can be done by changing the scan rate applied in the cyclic voltammogram.

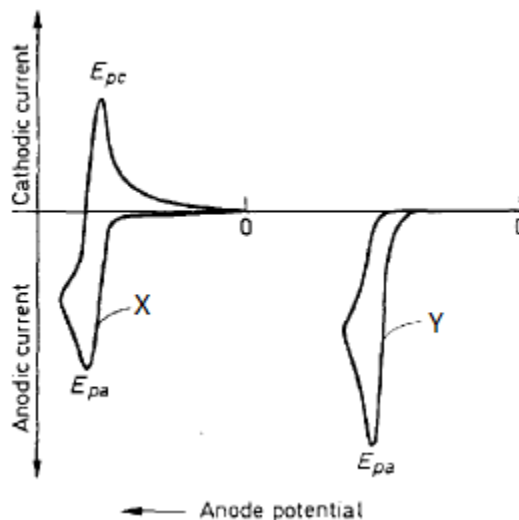


Figure 1.3: Cyclic voltammogram of reversible (curve X) and irreversible (curve Y) oxidation. The scan is initiated at the O or D point in the anodic direction and followed by the reversal of scan direction after passing the peak potential (E_{pa}). (Ebersson and Schäfer, 1971. p. 19)

1.5.2 Controlled Potential Electrolysis

Controlled potential electrolysis is the electrolysis that is run at a fixed potential. It is always run after the cyclic voltammetry once the redox potential is identified. In controlled potential electrolysis, only the substrate is being oxidized or reduced and the current will decrease as time increases. The substrate is consumed over time and less substrate will be available for the reaction. Thus the number of electrons transferred per unit time is decreased, resulting in the decrease of current. The end point of the electrochemical reaction is recognized as the current

decreases to a significant low value (background current). Decomposition process of solvent-supporting electrolyte would not take place since it requires a higher potential than the substrate.

1.5.3 Coulometry

Coulometry gives a graph of current (in A) against time (in s) resulted from the controlled potential electrolysis. By integrating the graph, the total amount of charge (in C) needed for the electrochemical reaction of the substrate can be known. As a result, the number of electrons transferred per substrate molecule can be calculated by the following formula deduced from the Faraday's law:

$$Q = nFM$$

Q = The total amount of charge (in C)

n = Number of electrons transferred per substrate molecule

F = Faraday constant (96485 C mol⁻¹)

M = Number of moles of the substrate reacted

1.6 Components of Electrochemical Cell

An electrochemical cell is composed of a glass cell and a Teflon cap with working, counter and reference electrodes as well as inert air purge line immersed into a

solution containing substrate and supporting electrolyte. Other than that, the three electrodes are connected to a potentiostat.

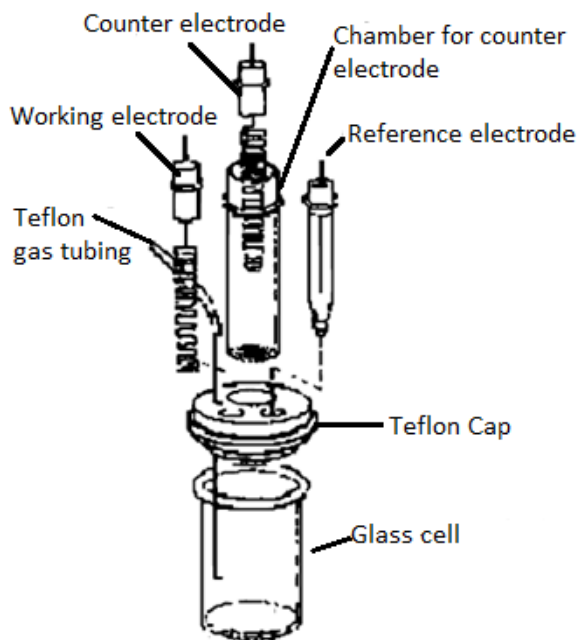


Figure 1.4: Typical setup of an electrochemical cell. (Núñez-Vergara, et al., 1999, p. 1484)

A working electrode is responsible for facilitating the charge transfer to and from the substrate. A counter electrode is responsible for completing the circuit by balancing the charge added or removed by the working electrode. A reference electrode is used to measure the potential of the working electrode. Basically, there is no current flowing through the reference electrode because its potential must remain unchanged. The supporting electrolyte solution containing mobile electrically charged ions functions as the carrier of electric current.

In fact, the electrolyte solution has to be purged with inert gas, such as argon or nitrogen before measurements are started in order to remove dissolved oxygen from the solution. Otherwise, oxygen may be reduced or could react with radical cations or anions produced at the electrode, resulting in the formation of undesired products (Lund and Hammerich, 2001).

1.6.1 Working Electrode

Generally, the working electrodes with a high signal to noise ratio and the reproducible response are desired. The selection for working electrode depends mainly on two parameters which are the redox property of the substrate and the ratio of background current to the potential region needed for the measurement. Working electrodes can be made from metals (platinum or gold), metal oxides, carbon, and some polymers. A wire, a disc, a small plate or a sphere is the common geometry of the working electrode. The geometric area is generally in the range of 0.01 cm^2 to 1.00 cm^2 (Pletcher, 2009).

1.6.2 Counter Electrode

A counter electrode is used to provide an equal magnitude current while in opposite sign corresponding to the current at the working electrode. For example, as oxidation takes place at the working electrode, reduction will then happen at the non-isolated counter electrode and vice versa. The magnitude of charge that

passes through the working electrode and the counter electrode will be equal. (Pletcher, 2009) Platinum, carbon, nickel or steel are some of the material for counter electrode with carbon and platinum are the most commonly used materials.

1.6.3 Reference Electrode

A reference electrode is used to control the potential at the working electrode. This is the main difference between a simple electrochemical cell (two-electrode cell consists of cathode and anode) with the electrochemical cell (three-electrode cell) for controlled potential electrolysis. In the controlled potential electrolysis, a fixed potential must remain constant throughout the electrolysis. The reference electrodes commonly used are saturated calomel electrode (SCE) and silver-silver chloride electrode.

1.6.4 Electrolyte Solution

For most electrochemical studies, the solution contains a large excess of an electrolyte. Pletcher (2009) revealed that this has several functions:

- To provide the solution ionic conductivity and hence lower its resistance.
- To serve as an ion source for the formation of double layer at the electrode surface.

- To prevent migration possessing an important role in the mass transport of the substrate or the product of electron transfer. Migration is the mechanism of charge passing through the solution.
- Contribute to the ionic strength of the medium.
- To function as a buffer in order to prevent a pH change within the reaction layer at the electrode surface. The change of pH is due to the H^+ or OH^- is being produced or consumed during the electron-transfer reaction.

1.6.5 Separators and Membranes

It is preferable to isolate the counter electrode and the reference electrode in most cases in order to prevent undesirable reactions occur at the surface of the reference or counter electrode. The separators allow the transport of cations or anions but not the substrate. The examples of separator are porous ceramics, glass sinters, porous polymers or ion-permeable membranes. Since there is no current flowing through the reference electrode, so the resistance of the separator between the working and reference electrode is not an issue. Therefore, ceramics with low porosity are used as the separators between the two electrodes. In order to have a uniform current path between the counter and working electrode, the separators should possess a larger area than that of the electrodes. Commonly, the separators are glass sinters or ion-permeable membrane. (Pletcher, 2009)

1.7 Microwave-Assisted synthesis

Microwave-assisted synthesis is the use of microwave energy to conduct chemical reactions. Microwaves have frequency of 0.3 to 300 GHz and wavelength of 1mm to 1m in the electromagnetic spectrum. They lie between radio wave and infrared frequencies in the electromagnetic radiation region. Unlike traditional chemical synthesis using conductive heating, the energy is directly transferred to the reactants in microwave-assisted synthesis, causing a rapid increase in the temperature of reaction mixture and thus shortening reaction time.

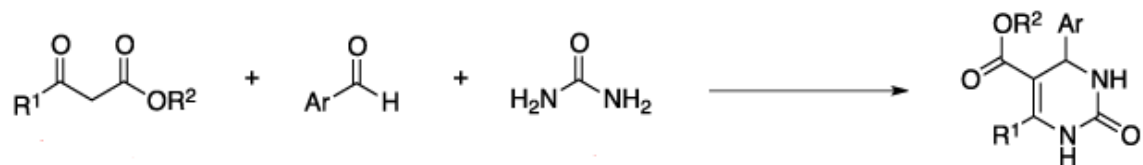
In conductive heating, heat has to pass through the walls of the vessel before it is applied to the solvent and reactants. This type of heating is time-consuming since it depends on the thermal conductivity of the materials. Besides that, it causes the temperature of the vessel to be greater than that of the reactants and solvent inside at the beginning of heating. It takes time for the vessel and reaction mixture to reach thermal equilibrium. Other than that, the heat source has to be removed and the reaction mixture cooled subsequently to reduce the internal bulk temperature. Thus, the internal bulk temperature is hard to control over the reaction. (Hayes, 2002)

In the past few years, microwave heating has been proved to increase product yield and improve product purities by minimizing undesired side reactions. Furthermore, microwave-assisted synthesis is more environmental friendly

compared to traditional chemical reaction due to less energy, solvents, and reagents are required.

1.8 Biginelli Reaction

Biginelli reaction is a three component reaction that produces 3,4-dihydropyrimidin-2(1*H*)-one from a β -keto ester, an aryl aldehyde, and urea. It was discovered by the Italian chemist, Pietro Biginelli in 1893. The 3,4-dihydropyrimidin-2(1*H*)-one was made by refluxing benzaldehyde, ethylacetoacetate, and urea in ethanol. The reaction was catalyzed by hydrochloric acid. After the reaction was ended, a solid crystalline product was obtained upon cooling. Throughout the years, many researchers have carried out this reaction in order to improve the yield by modifying the catalyst and reaction condition. The interest and popularity of 3,4-dihydropyrimidin-2(1*H*)-ones is because of their wide range of biological activities, such as antibacterial, antitumor, and antiviral, resulting in therapeutic and pharmaceutical applications (Pasha, Swamy and Jayashankara, 2005).



Scheme 1.5: Biginelli reaction of β -keto ester (R^1 and R^2 are alkyl groups), aryl aldehyde, and urea.

1.9 Objectives of Study

The objectives of this study are listed below:

- To synthesize 5-ethoxycarbonyl-6-methyl-4-(*p*-tolyl)-3,4-dihydropyrimidin-2(1*H*)-one for electrochemical analysis.
- To establish the electrochemical properties of 3,4-dihydropyrimidin-2(1*H*)-one.
- To separate the products of electrolysis by chromatographic methods.
- To characterize the products by exhaustive spectroscopic analysis.

CHAPTER 2

LITERATURE REVIEW

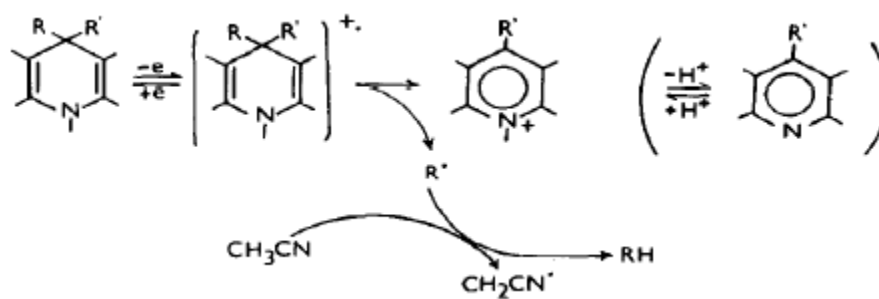
2.1 Electrochemical Studies of Heterocyclic Amines

Heterocyclic amines are defined as a molecule carrying a cyclic structure containing at least one nitrogen atom and probably with other additional heteroatoms, such as oxygen, or sulphur (Lawrence, 2004). Heterocyclic amines, such as pyridines, pyrimidines, and pyrimidinones show significant importance in pharmaceutical and industrial usages. The electrochemical studies of heterocyclic amines are important in order to understand the basic trend of selective redox position of the functional groups that exist in the substrate to be investigated.

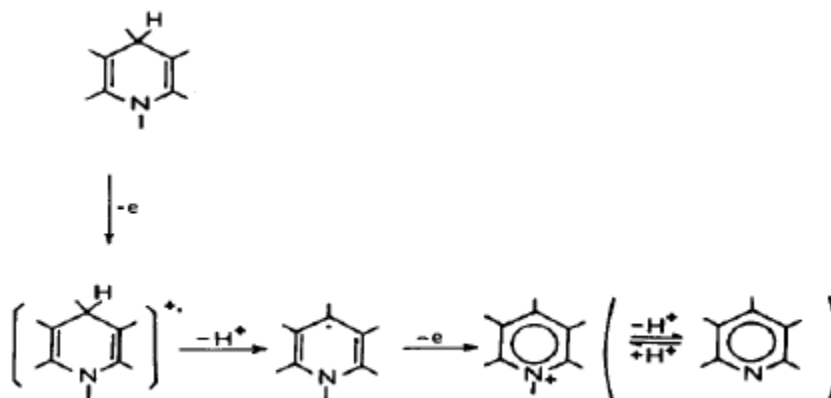
2.1.1 Pyridines

The mechanism of electrochemical oxidation of 1,4-dihydropyridine derivatives in acetonitrile has been established by Ludvík, Volke and Klíma in 1987. The types of 1,4-dihydropyridines derivatives investigated including PyH and PyR type. The PyH type is the substituted 1,4-dihydropyridines that possess at least one hydrogen atom at the position 4. Whereas the PyR type is the 1,4-dihydropyridine derivatives with a completely substituted position 4. The study was carried out using platinum as working electrode with acetonitrile as solvent.

Based on the mechanism proposed by Ludvík, Volke and Klíma (1987), the PyR derivatives are oxidized in a single-electron mechanism and forming a radical cation $\text{PyR}^{\bullet+}$, and followed by the loss of the substituent at position 4 as a radical to form cation Py^+ . (Scheme 2.1) In comparison, two-electron transfer is involved in the oxidation of PyH derivatives. The first electron transfer results in the formation of a radical cation $\text{PyH}^{\bullet+}$ and followed by the loss of one proton to form the radical Py^\bullet . The cation Py^+ is then formed by the subsequent electron transfer. (Scheme 2.2)



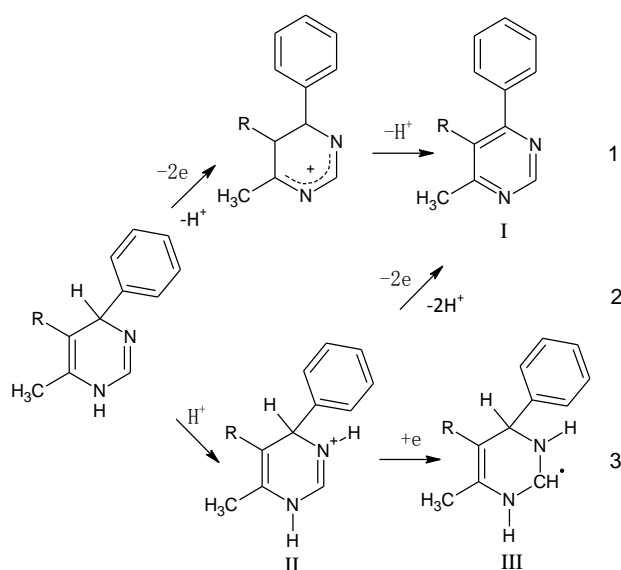
Scheme 2.1: Mechanistic pathway of electrochemical oxidation of PyR derivatives, where R and R' represent the alkyl group. (Ludvík, Volke and Klíma, 1987. p. 1068)



Scheme 2.2: Anodic oxidation mechanism of PyH derivatives. (Ludvík, Volke and Klíma, 1987. p. 1070)

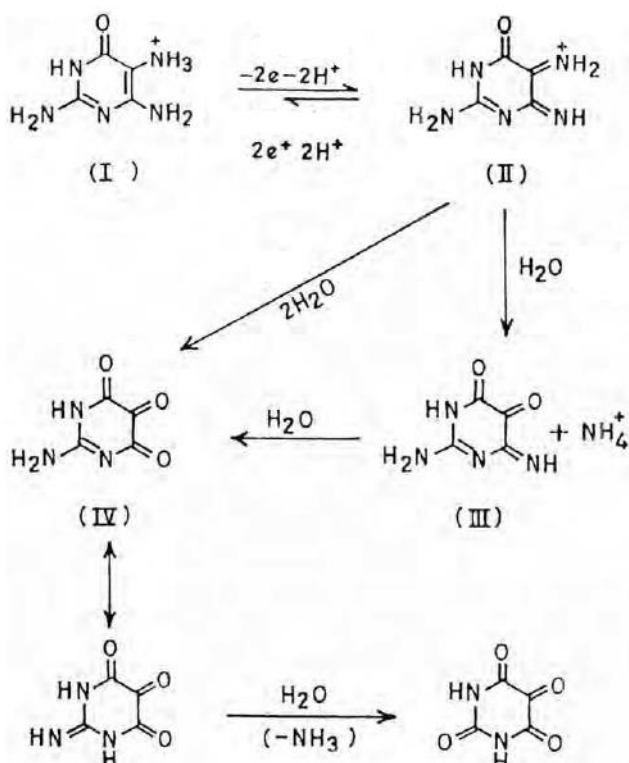
2.1.2 Pyrimidines

Kadysh, et al. (1989) have performed their study on electrochemical oxidation and reduction of 4-aryl-1,4-dihydropyrimidines in acetonitrile. The study was carried out using carbon as working electrode and platinum as counter electrode. The reference electrode used was a silver-silver nitrate electrode. A total of two electrons are involved in the anodic oxidation of the protonated and non-protonated 1,4- dihydropyrimidines. The protonation is because of the addition of proton formed during route 1. The protonated 1,4- dihydropyrimidines II also will be oxidized to the end product I through route 2. Besides that, the protonated 1,4- dihydropyrimidines II could be reduced to the intermediate III through route 3. The intermediate then goes through dimerization to give a dimer. The mechanism proposed is shown in Scheme 2.3.



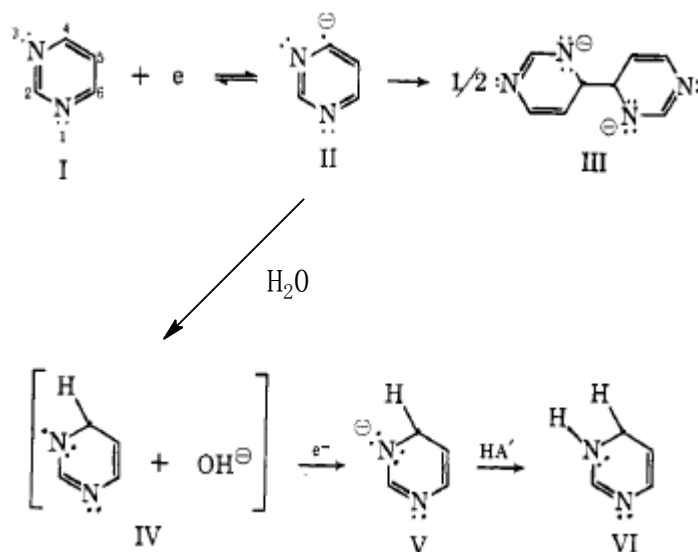
Scheme 2.3: Mechanistic pathway of electrochemical oxidation and reduction of 4-aryl-1,4-dihydropyrimidines, where R represents the ethoxy, acetyl, and nitryl substituent groups.

In 1999, Goyal, et al. reported the mechanistic pathway of electrochemical oxidation of 6-hydroxy-2,4,5-triaminopyrimidine I in phosphate buffer at pyrolytic graphite electrode. The counter electrode and reference electrode used were platinum and saturated calomel electrode, respectively. The electrochemical oxidation of 6-hydroxy-2,4,5-triaminopyrimidine I is a two-electron oxidation. The diimine II produced from the electrode reaction of 6-hydroxy-2,4,5-triaminopyrimidine I is highly unstable, and hence it easily undergoes hydrolysis to give the intermediate IV and ammonia. The ammonia is converted to ammonium ion in acidic condition. The hydrolysis occurs in two steps by forming quinoneimine III. The subsequent hydrolysis and deamination result in the formation of the end product alloxan. (Scheme 2.4)



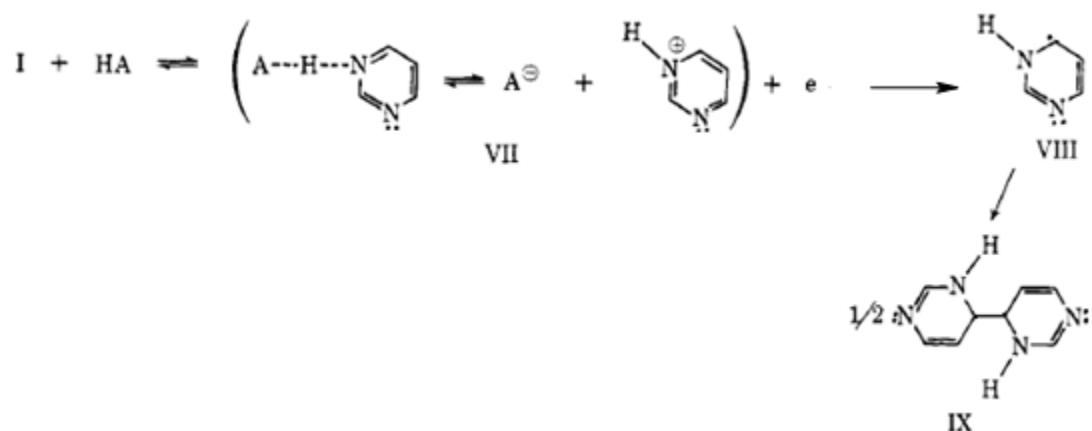
Scheme 2.4: Proposed mechanism of anodic oxidation of 6-hydroxy-2,4,5-triaminopyrimidine. (Goyal, et al., 1999, p. 1022)

The cathodic reductions of pyrimidine in acetonitrile have been studied by O'Reilly and Elving in 1971. The electrochemical reduction was carried out at mercury electrode. The reference electrode used was a silver-silver nitrate electrode and the counter electrode was a platinum foil. Mechanistically, the one-electron reduction of pyrimidine I provide a radical anion II. The addition of electron to pyrimidine I occurs at the position 4. The radical may go through dimerization to form dimer III or proton transfer with residual water (10 mM) at the position 4 to form the intermediate IV and followed by a rapid electron transfer and protonation to form the dihydropyrimidine V. The HA' refers to any proton source, such as residual water. (Scheme 2.5)



Scheme 2.5: Electrochemical reduction mechanism of pyrimidine with proton source at concentration of 10 mM. (O'Reilly and Elving, 1971. p. 1878)

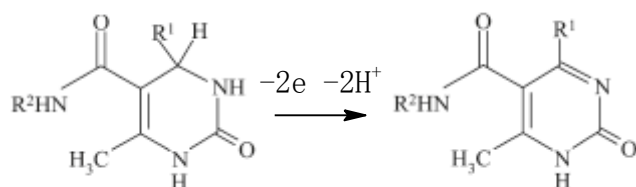
O'Reilly and Elving also studied the electrochemical reduction of pyrimidine with sufficient proton source, residual water at concentration 100 mM, using the same electrochemical cell setup. The pyrimidine I will be firstly protonated by the residual water to give an intermediate VII. This intermediate VII then undergoes one-electron addition to C-4 position forming a radical anion VIII. The radical anion VIII then goes through rapid dimerization to give the pyrimidine dimer IX. In conclusion, a higher concentration of proton source will lead to a different mechanistic pathway. (Scheme 2.6)



Scheme 2.6: Mechanism of electrochemical reduction of pyrimidine with proton source at concentration of 100 mM. (O'Reilly and Elving, 1971. p. 1878)

2.1.3 Pyrimidinones

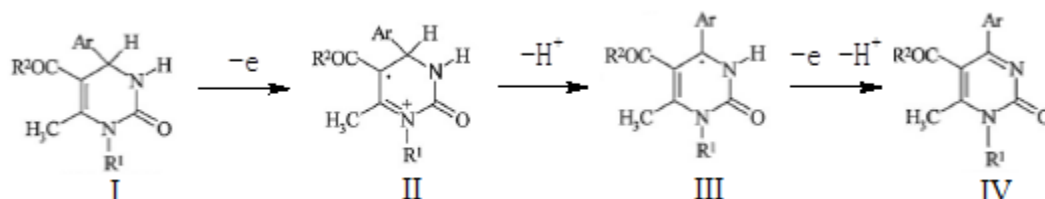
Memarian, et al. (2011) have studied the voltammetric oxidation of 2-oxo-1,2,3,4-tetrahydropyrimidin-5-carboxamides in acetonitrile. They performed the electrochemical experiments in a three-electrode electrochemical cell and using carbon as working electrode and platinum as counter electrode. The reference electrode used was a silver electrode. The oxidation is a $2e-2H^+$ reaction (Scheme 2.7). In conclusion a change in the R^1 and R^2 substituent groups will not affect the formation of the end product.



Scheme 2.7: Voltammetric oxidation of 2-oxo-1,2,3,4-tetrahydropyrimidin-5-carboxamides, where R^1 is the aryl group and R^2 is the alkyl group. (Memarian, et al., 2012. p. 8266)

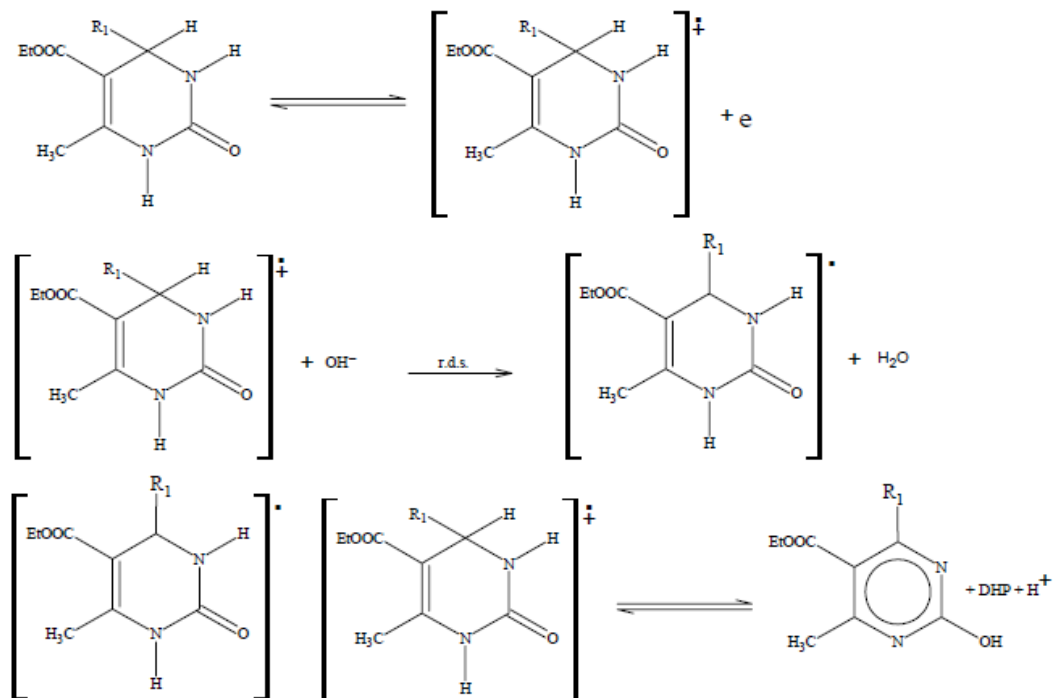
Similar research has been published by Memarian, et al. in 2012 regarding the mechanistic pathway of electrochemical oxidation of 2-oxo-1,2,3,4-tetrahydropyrimidines in acetonitrile and alcohol. The electrochemical cell setup was the same with what has been described previously. They found that the mechanistic pathway will not be affected by changing the solvent. The electrochemical oxidation is still a $2e-2H^+$ reaction. The mechanism proposed by Memarian et al. is shown in Scheme 2.8. The initial electron transfer from the pyrimidinone I will form the radical cation II. The radical cation II is then

transformed into the cation III by losing one proton at position C-4. The end product IV is formed from the cation III after a loss of an electron and proton.

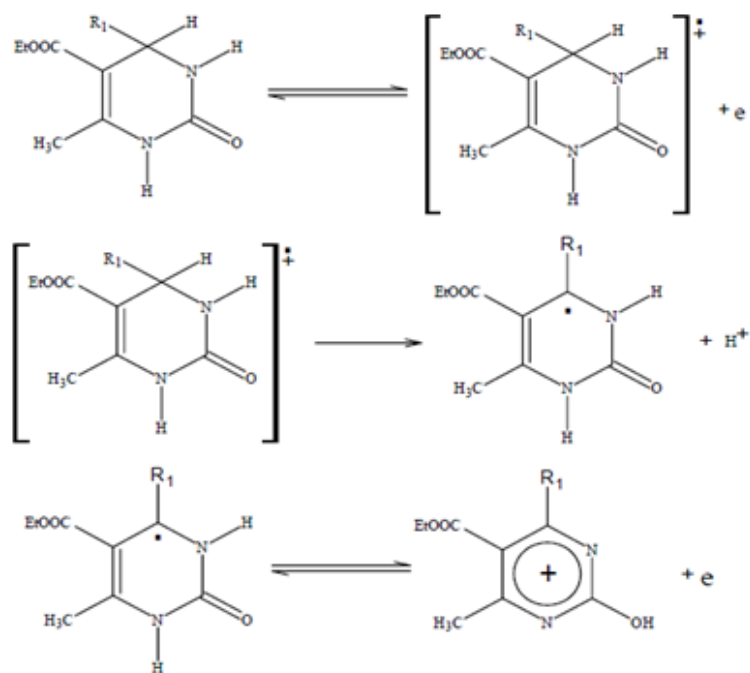


Scheme 2.8: Mechanism of anodic oxidation of 2-oxo-1,2,3,4-tetrahydropyrimidines, where R¹ represents the hydrogen, methyl, and phenyl substituent; R² indicates the ethoxy, methoxy, methyl, and phenyl substituent. (Memarian, et al., 2012. p. 1005)

Aceves, Miranda and Kappe (2007) have established the mechanism of electrochemical oxidation of various dihydropyrimidinones (DHPs) in acidic and basic media. The study was performed using platinum as working electrode with acetonitrile as solvent. The counter electrode used was a stainless steel wire and the reference electrode was silver-silver nitrate. The electrochemical oxidation of the DHPs in basic medium involves one-electron transfer. In contrast, the electrochemical oxidation in acidic medium is a two-electron process. The end product resulted from the oxidation in acidic medium is found as a form of salt in solution. In basic medium, the mechanism follows the ECE sequence, where E is the electrode process and C is the chemical process (Scheme 2.9). In acidic medium, the mechanism follows the ECC sequence (Scheme 2.10). Both the oxidations in basic and acidic media involve the removing of proton at C-4 position of the pyrimidinone ring.

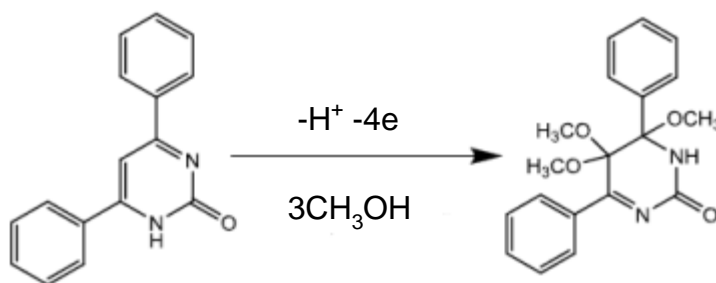


Scheme 2.9: Mechanism of electrochemical oxidation of DHPs in basic medium, where R_1 represents the aryl substituent group. (Aceves, Miranda and Kappe, 2007. p. 53)



Scheme 2.10: Proposed mechanism of electrochemical oxidation of DHPs in acidic medium, where R_1 represents the aryl substituent group. (Aceves, Miranda and Kappe, 2007. p. 54)

The electrochemical oxidation of 4,6-diphenylpyrimidin-2(1*H*)-one in methanol has been investigated by Lee (2012). The studied was carried out in a three-electrode cell equipped with carbon working electrode, non-isolated platinum counter electrode, and silver-silver chloride reference electrode. The oxidation is a 4e-H⁺ reaction (Scheme 2.11). A total of three methoxy groups are attached to the pyrimidinone ring at the end of the reaction.



Scheme 2.11 Electrochemical oxidation of 4,6-diphenylpyrimidin-2(1*H*)-one. (Lee, 2012. p. 51)

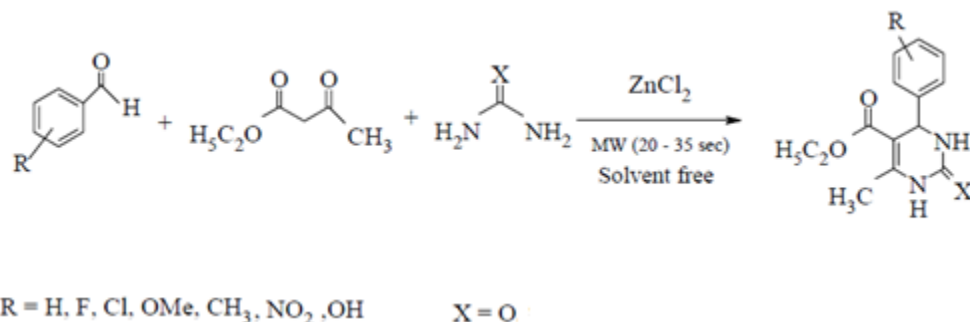
2.2 Microwave-Assisted Synthesis of 3,4-Dihydropyrimidin-2(1*H*)-ones

Microwave-assisted synthesis is considered as a new technique for synthesis because of its ability to speed up the reaction and providing a high yield. Several studies of applying microwave technique to synthesize 3,4- dihydropyrimidin-2(1*H*)-ones will be discussed in this section. The articles reviewed prove that microwave synthesis method gives a fairly good yield and shorter reaction times.

In 2004, Mirza-Aghayan, Bolourtchian and Hosseini have proposed a new protocol to synthesize 3,4- dihydropyrimidin-2(1*H*)-ones from an aryl aldehyde, a

β -keto ester, and urea using ferric chloride hexahydrate as catalyst. Microwave irradiation has been used to speed up the synthesis of 3,4-dihydropyrimidin-2(1*H*)-ones. The reaction was performed in solvent-free condition with reaction times (20-30 sec), giving a good yield (40-68%).

Similar research has been published by Pasha, Swamy and Jayashankara in 2005 regarding synthesis of 3,4-dihydropyrimidin-2(1*H*)-ones using microwave technique. The reactions were catalyzed by zinc chloride. Moreover, the reaction was carried out in solvent-free condition and went to completion within 20-35sec, providing a high percentage yield (90-95%). (Scheme 2.12)



Scheme 2.12 Synthesis of 3,4-dihydropyrimidin-2(1*H*)-ones under microwave irradiation. (Pasha, Swamy and Jayashankar, 2005. p. 824)

CHAPTER 3

MATERIALS AND METHODS

3.1 Chemicals

Table 3.1: List of chemicals

Chemical	Source
Acetone*	QRċC
Acetonitrile*	RCI Labscan
Chloroform*	Fisher Scientific
Deuterated Chloroform*	MERCK
Ethyl Acetate*	Fisher Scientific
Ethyl Acetoacetate	MERCK
Ethyl Alcohol 95%(v/v)*	SYSTEM
Methanol*	Fisher Scientific
Methanol (LCMS Grade)	Fisher Scientific
Silica Gel 60 PF ₂₅₄ Containing Gypsum	MERCK
Tetraethylammonium Perchlorate*	NACALAI TESQUE
TLC Silica Gel 60 F ₂₅₄	MERCK
Urea*	SYSTEM
Zinc Chloride*	QRċC

*Chemicals are analytical reagent grade.

All chemicals were used as received without further purification.

3.2 Instrumentation

Table 3.2: List of instruments

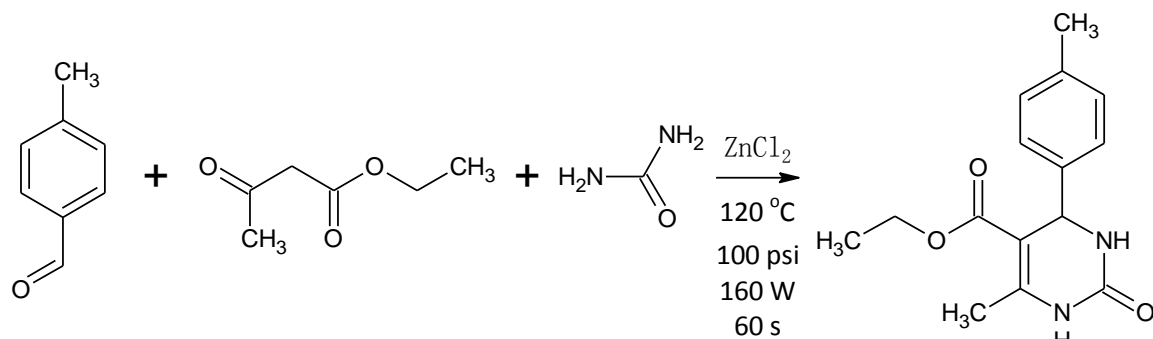
Instrument	Source, Model
HRESIQ-TOFLC/MS	Agilent Technologies, G6520B
Chromatotron	Harrison Research
FTIR Spectrometer	PerkinElmer, Spectrum RX I
Melting Point Apparatus	Stuart, SMP10
Microwave Synthesizer	CEM, Discover SP
400 MHz NMR Spectrometer	JEOL, JNM-ECX400
Potentiostat	Princeton Applied Research, 263A
Rotary Evaporator	BÜCHI, R-200

3.3 Experimental Procedure

3.3.1 Microwave-Assisted Synthesis of 5-Ethoxycarbonyl-6-methyl-4-(*p*-tolyl)-3,4-dihydropyrimidin-2(1*H*)-one

A mixture containing 2 mmol of 4-methylbenzaldehyde, ethyl acetoacetate, and urea each was added into a 10 ml Pyrex tube for the one pot condensation reaction. 1 mmol of zinc chloride was added to catalyze the condensation reaction. The sealed Pyrex tube was then put into the microwave synthesizer and irradiated for 60 seconds with the conditions of temperature being set at 120 °C, pressure of 100 psi and power of 150 W. The microwave-assisted synthesis was performed with the microwave synthesizer connected to a computer and operated by Synergy software 1.59. After the end of irradiation, the Pyrex tube was cooled to room

temperature and the product was then extracted using ethyl acetate and filtered by using filter paper. After the solvent was removed by using rotary evaporator, the product was then recrystallized from ethanol.



Scheme 3.1: Synthesis of the 3,4-dihydropyrimidin-2(1H)-one catalyzed by zinc chloride.

3.3.2 Electrochemical Studies of 5-Ethoxycarbonyl-6-methyl-4-(*p*-tolyl)-3,4-dihydropyrimidin-2(1H)-one

Cyclic voltammetry and controlled potential electrolysis were performed with the potentiostat connected to a computer and operated by Electrochemistry PowerSuite software 2.58.

3.3.2.1 Cyclic Voltammetry

The cyclic voltammetry was performed in a three-electrode electrochemical cell equipped with glassy carbon rod working electrode, isolated platinum coil wire counter electrode, and silver-silver chloride reference electrode. Firstly, the cyclic voltammogram of the 0.1 M electrolyte solution in a 100 mL glass cell was

obtained. The electrolyte solution was prepared by dissolving tetraethylammonium perchlorate in a binary solvent. After that, the cyclic voltammetry scan of the electrolyte solution with 5 mg of the 3,4-dihydropyrimidin-2(1*H*)-one substrate added was performed. Lastly, the cyclic voltammogram of the resulting solution with potassium hydroxide added was obtained. In general, two vertexes potential (-2 V and +2 V) cyclic voltammetry were employed. A total of four scans were done with 1 V/s scan rate in the potential range between -2 V and +2 V.

3.3.2.2 Controlled Potential Electrolysis

The controlled potential electrolysis was performed in the electrochemical cell using a porous cylindrical carbon cage working electrode (4 cm diameter x 5 cm height), non-isolated platinum coil wire counter electrode, and silver-silver chloride reference electrode. Another 25 mg of the 3,4-dihydropyrimidin-2(1*H*)-one substrate with potassium hydroxide (4.39 mM) were dissolved in the solution. The controlled potential electrolysis was then started with the redox potential of the substrate. The electrolysis was terminated when the current remained unchanged.

3.3.2.3 Isolation and Purification

The products formed from the electrolysis were firstly isolated from the bulk solution containing the supporting electrolyte. It was done by evaporating the solvent under reduced pressure. Chloroform was then used to extract the products. After that, the dissolved products were drawn out from the flask and transferred to a sample vial. Thin layer chromatography was then carried out to evaluate the formation of products by comparing the retardation factor value of the products with the substrate. The solvent system used was chloroform to acetonitrile at the ratio of 4:1. The same solvent system would be used in the further isolation.

Further isolation was performed using thin layer centrifugal chromatography. The separation was carried out on a silica gel layer cast on a glass centrifugal plate. The silica gel layer was washed with the solvent and allowed to rotate until equilibrium achieved. The products were dissolved in minimum chloroform and introduced into the flow dropwise. The solvent flow had to be stopped while introducing sample. After the sample was dried and coated on the silica layer, the flow was then continued to separate and drain out the product. The eluent was collected in several fractions based on the appearance of concentric bands upon separation visualized under UV irradiation. Then further purification process was carried out if required.

The silica gel layer was prepared by making a slurry like mixture containing 50 g of silica gel (containing gypsum) and 100 mL of icy cold water. The mixture was then distributed evenly on a glass centrifugal plate and allowed to stand at the room temperature for 30 minutes. After that, it was put in an oven overnight with temperature setting not more than 60 °C. The plate was taken out from the oven on the next day. It had to be cooled to room temperature before further processes were carried out.

3.3.3 Characterization

3.3.3.1 Nuclear Magnetic Resonance (NMR) Spectroscopy

The sample was prepared by dissolving the product in deuterated chloroform and filled in a sample tube to a height of around 4 cm. It was then analyzed by the NMR spectrometer with TMS as the internal standard for ^1H NMR and ^{13}C NMR experiments. The generated spectra, such as ^{13}C NMR, ^1H NMR, DEPT, HMQC, HMBC, and NOESY provide significant information to propose the structure of the product.

3.3.3.2 High Resolution Electrospray Ionization Quadrupole-Time of Flight (HRESIQ-TOF) Liquid Chromatography Mass Spectrometry

The sample was prepared by dissolving the product in LCMS grade methanol for direct injection to the mass spectrometer. The fragmentor voltage was set at +175

V or +300 V. The generated spectrum provided useful information in determining the molecular formula of the compound.

3.3.3.3 Fourier Transform Infrared (FTIR) Spectroscopy

The sample was prepared by dissolving the product in anhydrous chloroform. It was then spread evenly on a potassium bromide glass to form a thin film for FTIR analysis. The generated FTIR spectrum was used to identify the functional groups in the compound.

CHAPTER 4

RESULTS AND DISCUSSION

4.1 Microwave-Assisted Synthesis of 5-Ethoxycarbonyl-6-methyl-4-(*p*-tolyl)-3,4-dihydropyrimidin-2(1*H*)-one

5-Ethoxycarbonyl-6-methyl-4-(*p*-tolyl)-3,4-dihydropyrimidin-2(1*H*)-one, **GWS001** was synthesized for electrochemical analysis. The 3,4-dihydropyrimidin-2(1*H*)-one was obtained as a pale yellow amorphous solid with melting point in the range of 215 °C to 216 °C. The retardation factor (R_f) of **GWS001** in the solvent system chloroform: acetonitrile (4: 1) was obtained as 0.38. The physical appearance, melting point, and R_f of **GWS001** are tabulated in the following table (Table 4.1).

Table 4.1: Physical appearance, melting point, and R_f of GWS001.

Code	Physical Appearance	Melting Point (°C)		R_f
		Observed	Literature ^a	
GWS001	Pale yellow amorphous solid	215-216	214-215	0.38

^aThe melting point was reported by Pasha, Swamy and Jayashankara in 2005.

HRESIMS gave a pseudo molecular ion at 275. 1385 $[M+H]^+$ for a molecular formula $C_{15}H_{18}N_2O_3$. Based on this formula, the double bond equivalent was

obtained as 8. The molecular formula and its corresponding molecular ion as well as double equivalent are listed in the following table (Table 4.2).

Table 4.2: Molecular formula and its respective molecular ion as well as double bond equivalent of GWS001 provided by HRESIMS.

Molecular Formula of GWS001	Molecular Ion [M+H] ⁺		Double Bond Equivalent
	Observed	Calculated	
C ₁₅ H ₁₈ N ₂ O ₃	275.1385	275.1390	8

In the FTIR spectrum, the absorption of N-H stretch was detected at wavenumber of 3232 cm⁻¹. The absorption peaks at wavenumber of 3112 cm⁻¹ and 2979 cm⁻¹ are due to the aromatic C-H stretch and the sp³ C-H stretch respectively. Besides that, the spectrum shows the strong absorption peak at wavenumber at 1706 cm⁻¹ indicating the C=O stretch. A pair of medium absorption at wavenumber of 1648 cm⁻¹ and weak absorption at 1458 cm⁻¹ represents the aromatic C=C stretch. The two medium absorption peaks at wavenumber of 1225 cm⁻¹ and 1089 cm⁻¹ indicate the C-O stretch and C-N stretch respectively. The wavenumbers and its corresponding vibration mode for the various functional groups of **GWS001** are listed in the following table (Table 4.3).

Table 4.3: FTIR spectrum interpretation of GWS001.

Wavenumber (cm⁻¹)	Vibration Mode
3232	N-H stretch
3112	Aromatic C-H stretch
2979	sp ³ C-H stretch
1706	C=O stretch
1648 & 1458	Aromatic C=C stretch
1225	C-O stretch
1089	C-N stretch

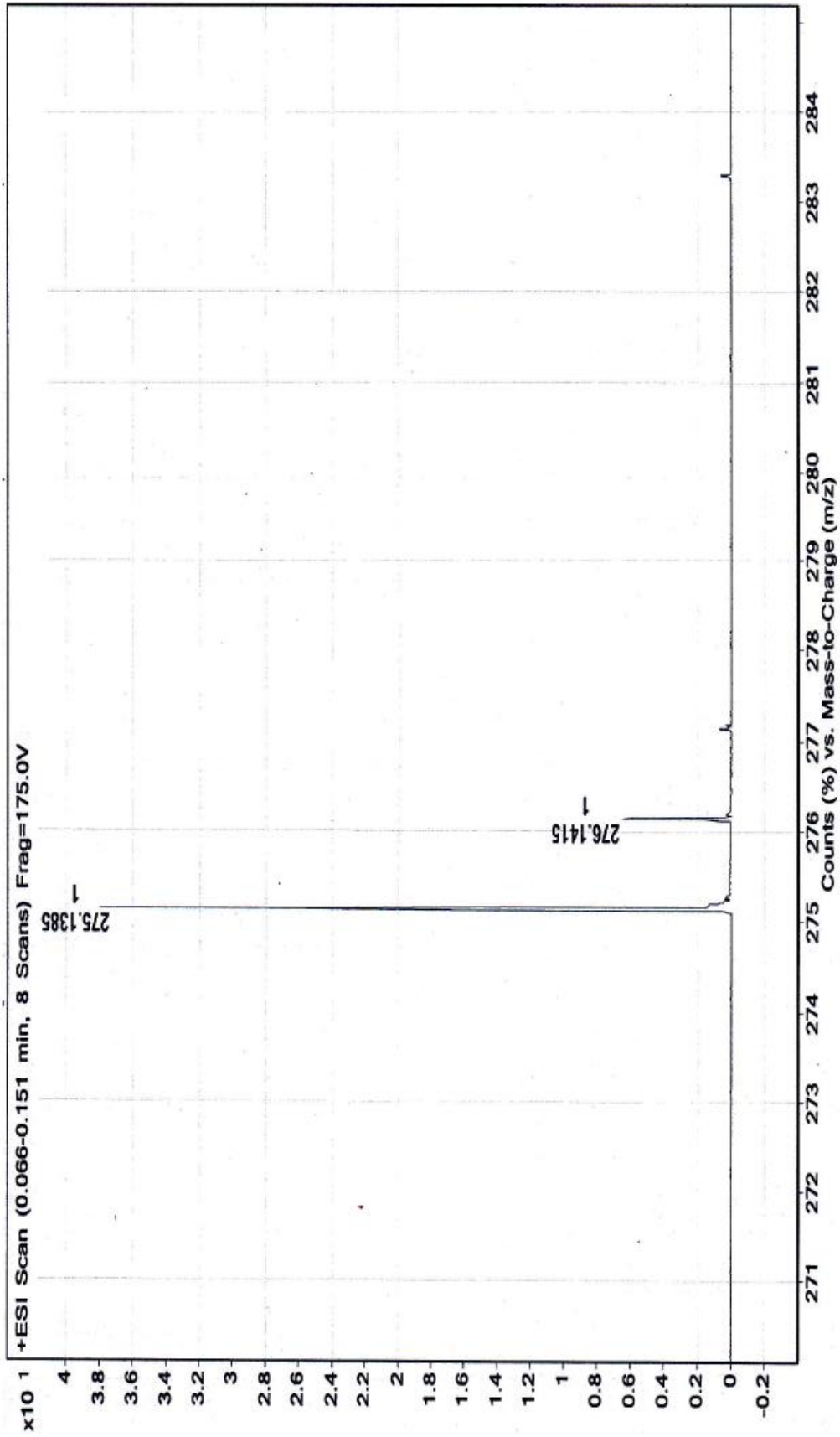


Figure 4.1: MS spectrum of GWS001.

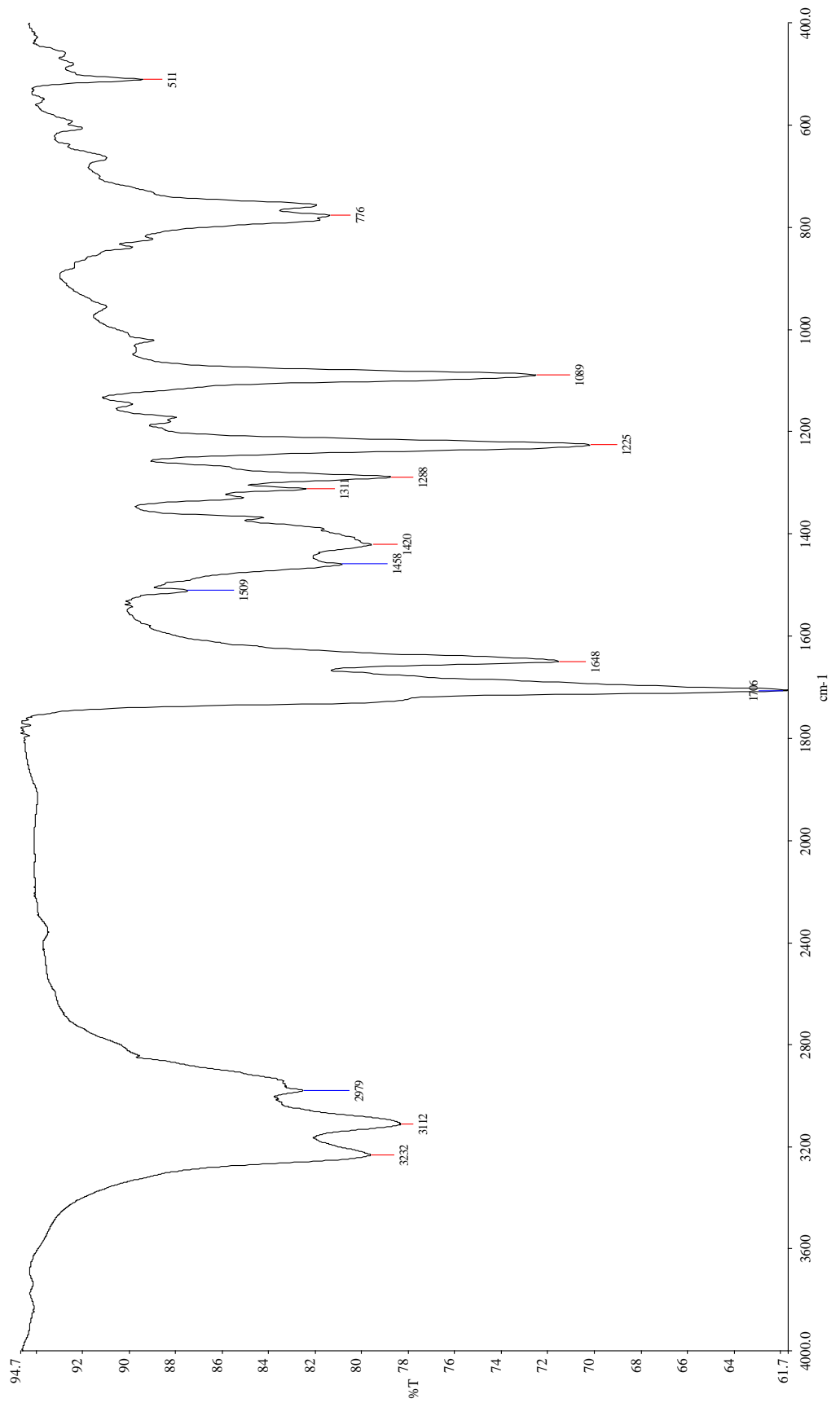


Figure 4.2: FTIR spectrum of GWS001 (thin film on KBr glass).

The structure of **GWS001** is shown as below in order to facilitate reference for discussion (Figure 4.3).

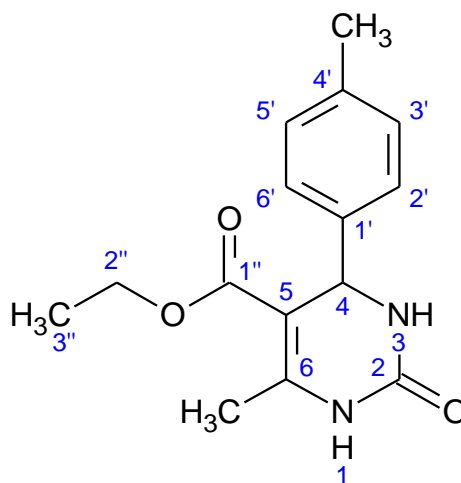


Figure 4.3: Structure of GWS001.

A total of 8 peaks were observed in the ¹H NMR spectrum. The two singlet peaks at δ 8.29 and δ 5.83 were assigned to H-1 and H-3, respectively. A pair of doublet peaks shown at the low field region represents the aromatic protons of a para-substituted aromatic ring. The doublet at δ 7.20 was attributed to the aromatic protons at H-2' and H-6', while the doublet at δ 7.10 was assigned to the aromatic protons at H-3' and H-5'. The doublet at δ 5.35 is derived from the proton at H-4 being adjacent to the proton at H-3. The deshielding effect of the atom is due to a coupling with an adjacent proton that is deshielded and was assigned to H-4. The quartet at δ 4.06 corresponds to the oxy-methylene protons at H-2''. The significant tallest peak observed at δ 2.32 belongs to the protons at 6-CH₃ and 4'-CH₃ together. The peak is caused by the overlapping of signals from

the two methyl groups. The triplet peaks appeared at δ 1.17 was assigned to the methyl group C-3''.

A total of 13 carbon signals were seen at the ^{13}C NMR spectrum. Nevertheless, there are actually 15 carbon atoms in the structure of **GWS001**. This is because of the overlapping of signals from the symmetrical methine carbons at the aromatic ring. The spectrum of the ^{13}C signals, there are 3 methyl carbons, 1 oxy-methylene carbon, 3 methine carbons, and 6 quaternary carbons. The two quaternary carbon peaks in the low field region at δ 165.6 and δ 153.4 are due to the ester group at position C-1'' and the amide group at position C-2, respectively. The C=O double bonds in the ester and amide group contribute to 2 double bond equivalents. The high chemical shift is because of the carbons are directly bonded to the electronegative oxygen atom, resulting in the strong inductive effect. Moreover, the sp^2 hybridization effect also contributes to the deshielding of the carbon nucleus resulting in the down field resonance.

The other quaternary peaks at δ 146.1, δ 140.7, and δ 137.5 were assigned to the unsaturated carbons at positions C-6, C-1', and C-4' respectively. The signal at δ 146.1 was assigned to the carbon at position C-6 due to its bonding to the electronegative nitrogen atom making it more deshielded. The two peaks at δ 129.2 and δ 137.5 indicate the methine carbons at the para-substituted aromatic ring. This aromatic ring contributes to 4 double bond equivalents. The peak at δ 129.2 was attributed to the aromatic ring carbons at position C-2' and C-6', while

the peak at δ 126.3 was assigned to the carbons at position C-3' and C-5'. The signal at δ 101.3 in the double bond region belongs to the carbon at position C-5. C-5 and C-6 carbons are double-bonded to each other and this contributes to 1 double bond equivalent. Thus, the last double bond equivalent to be accounted for is ascribed to the pyrimidinone ring. Besides that, the two signals at δ 59.8 and δ 55.2 are due to the oxy-methylene carbon at position C-2'' and the carbon at position C-4 respectively. The carbon at position C-2'' having higher chemical shift is because the carbon is attached to a more electronegative atom, oxygen, making it more deshielded.

The rest of peaks shown at the high field region are corresponding to the remaining saturated sp^3 carbons. The signals at δ 21.0 is resulted from the methyl carbon at position 4'-CH₃, while the peak at δ 18.5 is assigned to the methyl carbon at position 6-CH₃. The peak having δ 14.0 is due to the carbon at position C-3''. The methyl carbons at position 4'-CH₃ and 6-CH₃ possessing larger chemical shifts as compared to the carbon at position C-3'' is due to the anisotropic field of the nearby π electrons. The methyl carbon at position 4'-CH₃ has higher chemical shift than the carbon at 6-CH₃ is caused by a larger anisotropic field produced by the delocalization of the nearby π electrons in the aromatic ring. The chemical shifts of each carbon and proton for **GWS001** are listed in the following table (Table 4.4).

Table 4.4: NMR spectra interpretation of GWS001.

Position	δ (ppm), Multiplicity		Coupling Constant, J (Hz)
	^{13}C	^1H	
1	—	8.29, <i>s</i>	—
2	153.4, <i>s</i>	—	—
3	—	5.83, <i>s</i>	—
4	55.2, <i>d</i>	5.35, <i>d</i>	2.7
5	101.3, <i>s</i>	—	—
6	146.1, <i>s</i>	—	—
6-CH₃	18.5, <i>q</i>	2.32, <i>s</i>	—
1'	140.7, <i>s</i>	—	—
2' & 6'	129.2, <i>d</i>	7.20, <i>d</i>	8.2
3' & 5'	26.3, <i>d</i>	7.10, <i>d</i>	8.2
4'	137.5, <i>s</i>	—	—
4'-CH₃	21.00, <i>q</i>	2.32, <i>s</i>	—
1''	165.6, <i>s</i>	—	—
2''	59.8, <i>t</i>	4.06, <i>q</i>	7.3
3''	14.0, <i>q</i>	1.17, <i>t</i>	7.3

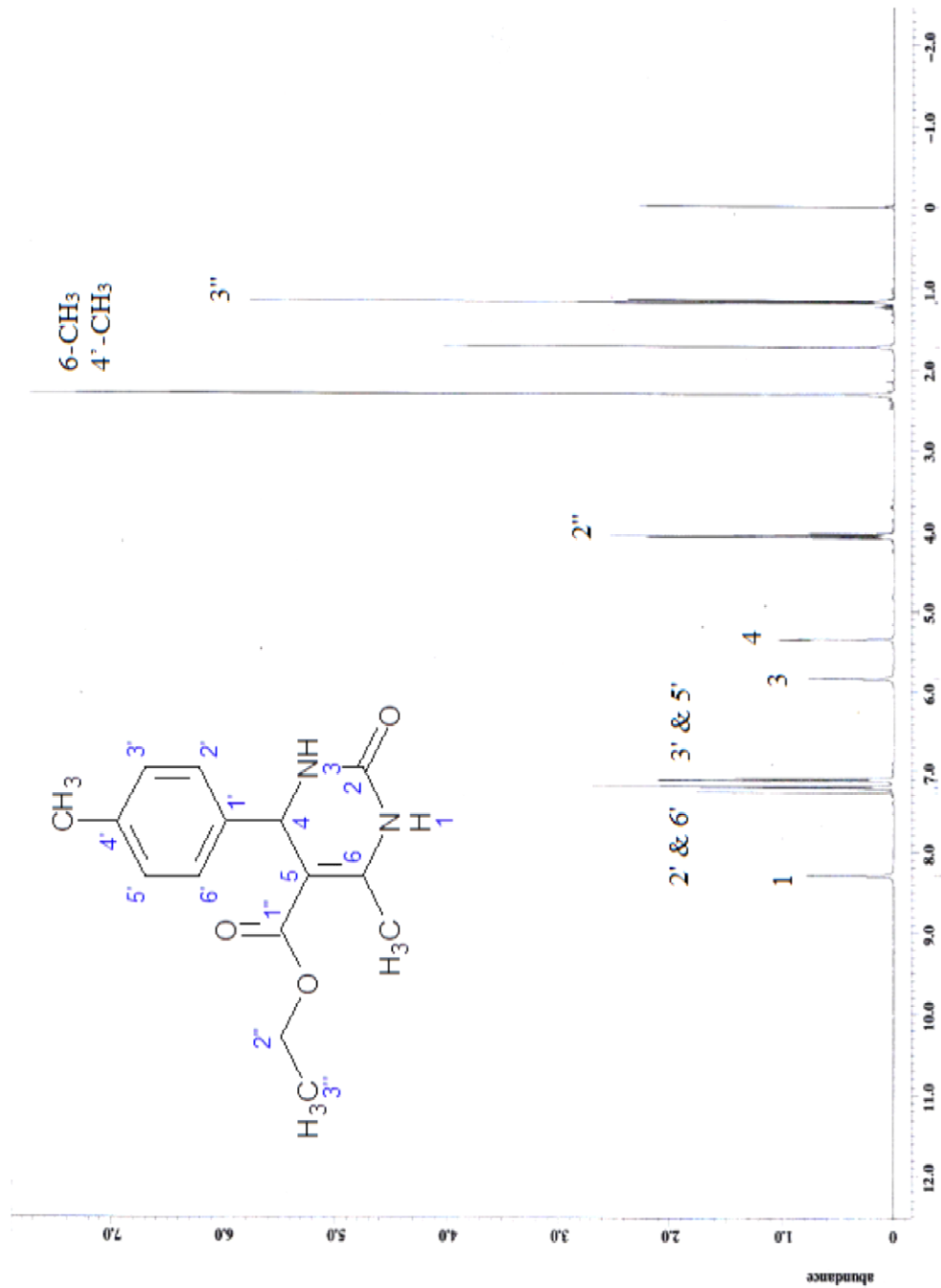


Figure 4.4: ^1H NMR spectrum of GWS001 in CDCl_3 (400 MHz).

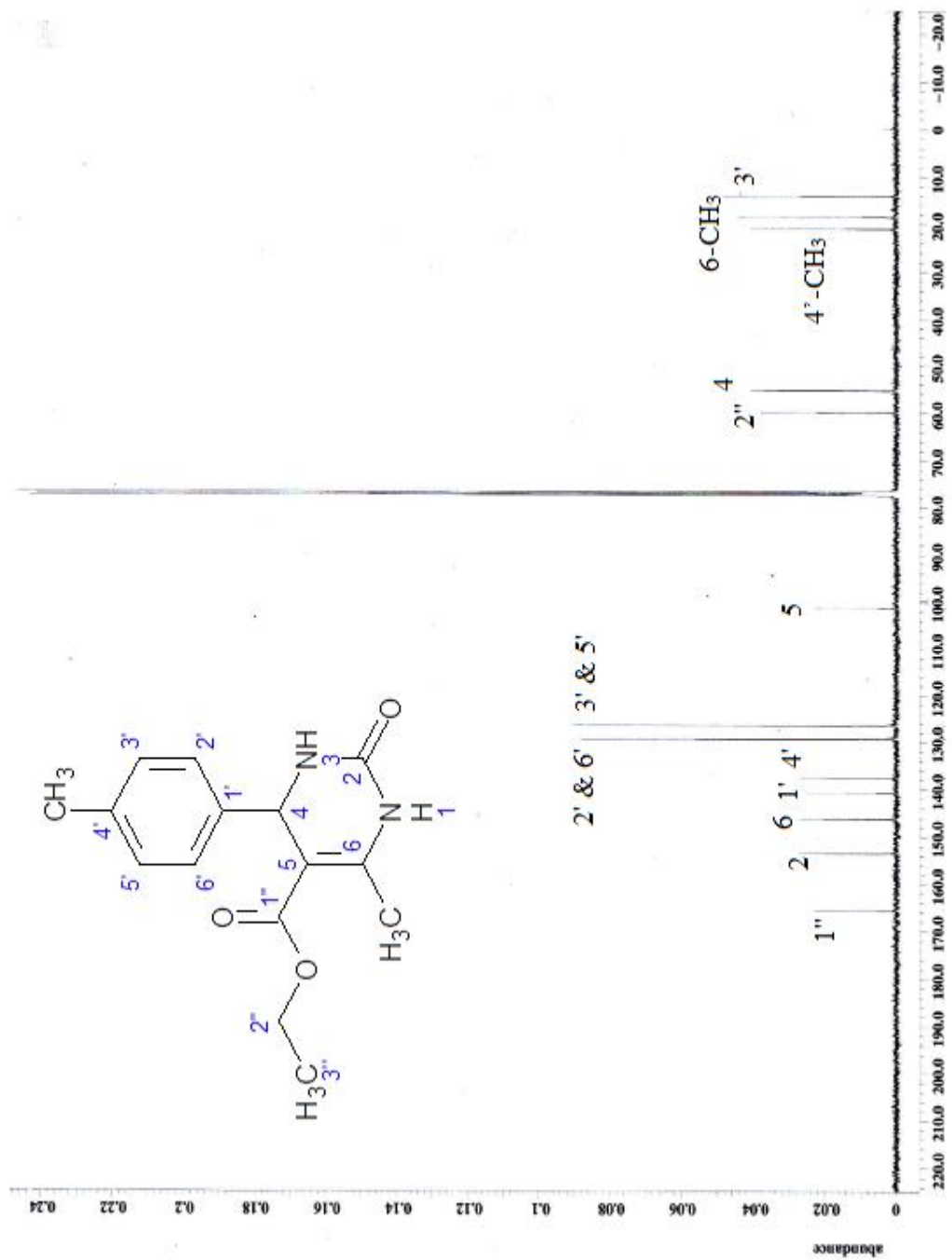


Figure 4.5: ^{13}C NMR spectrum of GWS001 in CDCl_3 (100 MHz).

4.2 Electrochemical Studies of 5-Ethoxycarbonyl-6-methyl-4-(*p*-tolyl)-3,4-dihydropyrimidin-2(1*H*)-one

Electrochemical studies of **GWS001** involved cyclic voltammetric studies and controlled-potential electrolysis using three solvent mixtures. The studies were firstly carried out using 80% acetonitrile-methanol in which the acetonitrile and methanol component were used to dissolve the supporting electrolyte and the substrate, **GWS001** respectively. Since the substrate was insoluble in acetonitrile, a minimum methanol was applied to the solvent system. The intermediates were expected having higher changes to be attacked by the nucleophile, methanol to give a different product with exchange of solvent composition to 50% acetonitrile-methanol. Lastly, the 50% methanol was replaced with acetone in order to study the effect of acetone on the reaction pathway. The results showed that the solvents might take part in the electrochemical reactions of **GWS001**. The results of cyclic voltammetric studies and controlled potential electrolysis are summarized in the flowing table (Table 4.5).

Table 4.5: Summary for the results of electrochemical studies.

Solvent Composition	Potential of Electrolysis (V)	Duration (Hours)	Number of Electrons Transferred Per Substrate Molecule	Total Isolated Weight (mg)	Weight and Yield of Interest Product
80% CH ₃ CN 20% CH ₃ OH	0.98	3.9	9	23.6	5 mg 17% GWS002
50% CH ₃ CN 50% CH ₃ OH	1.23	4.4	13	18.4	4.1 mg 12% GWS003
50% CH ₃ CN 50% (CH ₃) ₂ CO	1.18	2.8	5	16.2	5.3 mg 19% GWS004

4.2.1 Electrolysis of 5-Ethoxycarbonyl-6-methyl-4-(*p*-tolyl)-3,4-dihydropyrimidin-2(1*H*)-one in 80% Acetonitrile-Methanol

In the cyclic voltammetric study of **GWS001** in solvent composition of 80% acetonitrile with 20% methanol, the scan was started by an increase in potential from the origin towards the positive vertex, followed by the scan in the opposite direction with a decrease in potential. By comparing with the cyclic voltammogram of the blank, an additional oxidation peak at a potential of 1.42 V was shown in the voltammogram (Figure 4.6) indicating the electrochemical oxidation peak of **GWS001** in that solvent system. With the subsequent addition of potassium hydroxide, the peak was enhanced and shifted to a smaller potential of 0.98 V.

This shows that addition of base will promote the electrochemical reaction and making it to occur at lower potential. This suggests that the reaction involving the release of protons, and hence the nitrogen atoms in substrate **GWS001** will be protonated by these protons. As a result, the nitrogen atom at position N-1 will no longer have the lone pair electron to allow the electron transfer at the electrode. If the protons are not removed, the amount of substrate possessing free nitrogen atom at N-1 position will decrease as more protons are given out from the reaction of the substrate. Therefore, the electrochemical reaction will no longer be able to continue when all the remaining substrate gets protonated. By adding potassium hydroxide as a proton scavenger, the protons will be captured by the hydroxide ion and allows the reaction to proceed to completion.

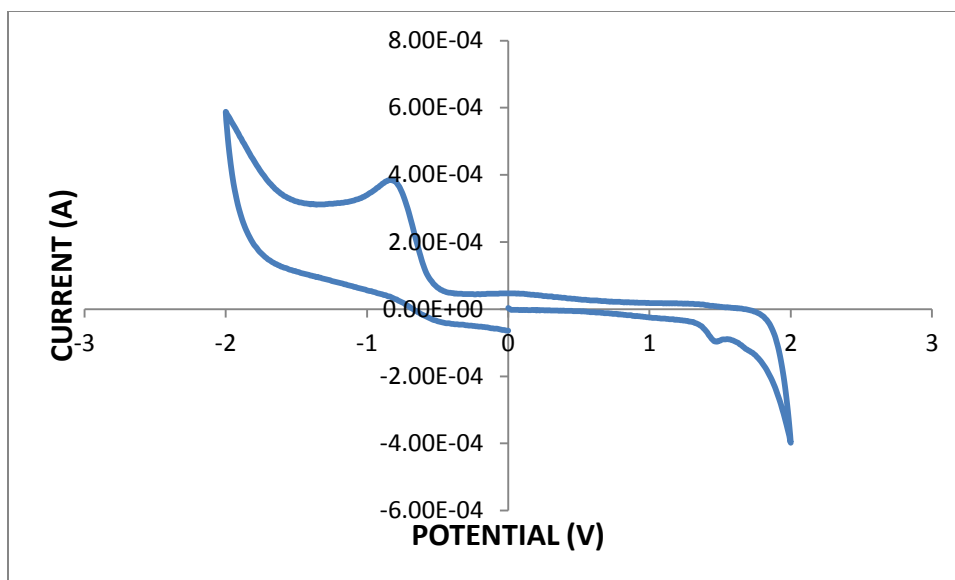


Figure 4.6: Cyclic voltammogram of GWS001 (5 mg) at glassy carbon rod working electrode, isolated platinum coil wire counter electrode, and silver-silver chloride reference electrode in 80% acetonitrile-methanol.

In the controlled potential electrolysis, the potential was set a little higher than the oxidation potential peak resulted from the addition of potassium hydroxide. This was to make sure that the substrate was fully consumed. The duration for the electrolysis of **GWS001** in solvent composition of 80% acetonitrile with 20% methanol was 14040 seconds. The number of electrons transferred per substrate molecule can be calculated using the formula derived from the Faraday's Law:

$$Q = nFM$$

where Q is the total amount of charge, n is the number of electrons transferred per substrate molecule, F is the Faraday constant (96485 C mol^{-1}), while M is the number of moles of the substrate reacted. The total amount of charge, Q can be obtained by integrating the graph of current, I (in A) versus time, t (in seconds) from the electrolysis of **GWS001** in that solvent composition,

$$Q = I \times t$$

$$= 92.7459 \text{ C}$$

Applying $Q = nFM$

$$M = \frac{29.1 \times 10^{-3} \text{ g}}{290.1630 \text{ g mol}^{-1}}$$

$$= 1.0029 \times 10^{-4} \text{ mol}$$

$$92.7459 \text{ C} = n(96485 \text{ C mol}^{-1})(1.0029 \times 10^{-4} \text{ mol})$$

$$n = \frac{92.7459 \text{ C}}{(96485 \text{ C mol}^{-1})(1.0029 \times 10^{-4} \text{ mol})}$$

$$= 9 \text{ electrons}$$

As a result, the electrochemical reaction of **GWS001** in solvent composition of 80% acetonitrile with 20% methanol involved 9 electrons transferred per substrate molecule. The total isolated crude weight of was 23.6 mg; however the weight of interest product, **GWS002** was only 5 mg with yield 17%. The other 15.6 mg was due to the substrate being converted to unwanted stuff during the electrolysis. The ^1H NMR spectrum of unwanted stuff is attached in the appendix.

GWS002 was obtained as a solid after the electrolysis. The retardation factor (R_f) of **GWS002** in the solvent system chloroform: acetonitrile (4: 1) was obtained as 0.22. HRESIMS gave a pseudo molecular ion at 273. 1223 $[\text{M}+\text{H}]^+$ for a molecular formula $\text{C}_{15}\text{H}_{16}\text{N}_2\text{O}_3$. This formula shows that **GWS002** has two hydrogen less than the starting material which the double bond equivalent has

increased one to nine. The molecular formula and its corresponding molecular ion as well as double equivalent are listed in the following table (Table 4.6).

Table 4.6: Molecular formula and its respective molecular ion as well as double bond equivalent of GWS002 provided by HRESIMS.

Molecular Formula of GWS002	Molecular Ion [M+H] ⁺		Double Bond Equivalent
	Observed	Calculated	
C ₁₅ H ₁₆ N ₂ O ₃	273.1223	273.1233	9

In the FTIR spectrum of **GWS002**, the absorption peaks at wavenumber 2925 cm⁻¹ is due to the sp³ C-H stretch. The ester C=O stretch was detected at the wavenumber of 1716 cm⁻¹. Besides that, the spectrum shows the strong absorption peak at wavenumber at 1658 cm⁻¹ indicating the amide C=O stretch. A pair of medium absorption at wavenumber of 1598 cm⁻¹ and weak absorption at 1434 cm⁻¹ indicates the aromatic C=C stretch. The medium absorption peaks at wavenumber of 1278 cm⁻¹ indicate the C-O stretch. The wavenumbers and its corresponding vibration mode for the various functional groups of **GWS002** are listed in the following table (Table 4.7).

Table 4.7: FTIR spectrum interpretation of GWS002.

Wavenumber (cm⁻¹)	Vibration Mode
2925	sp ³ C-H stretch
1716	Ester C=O stretch
1658	Amide C=O stretch
1598 & 1434	Aromatic C=C stretch
1278	C-O stretch

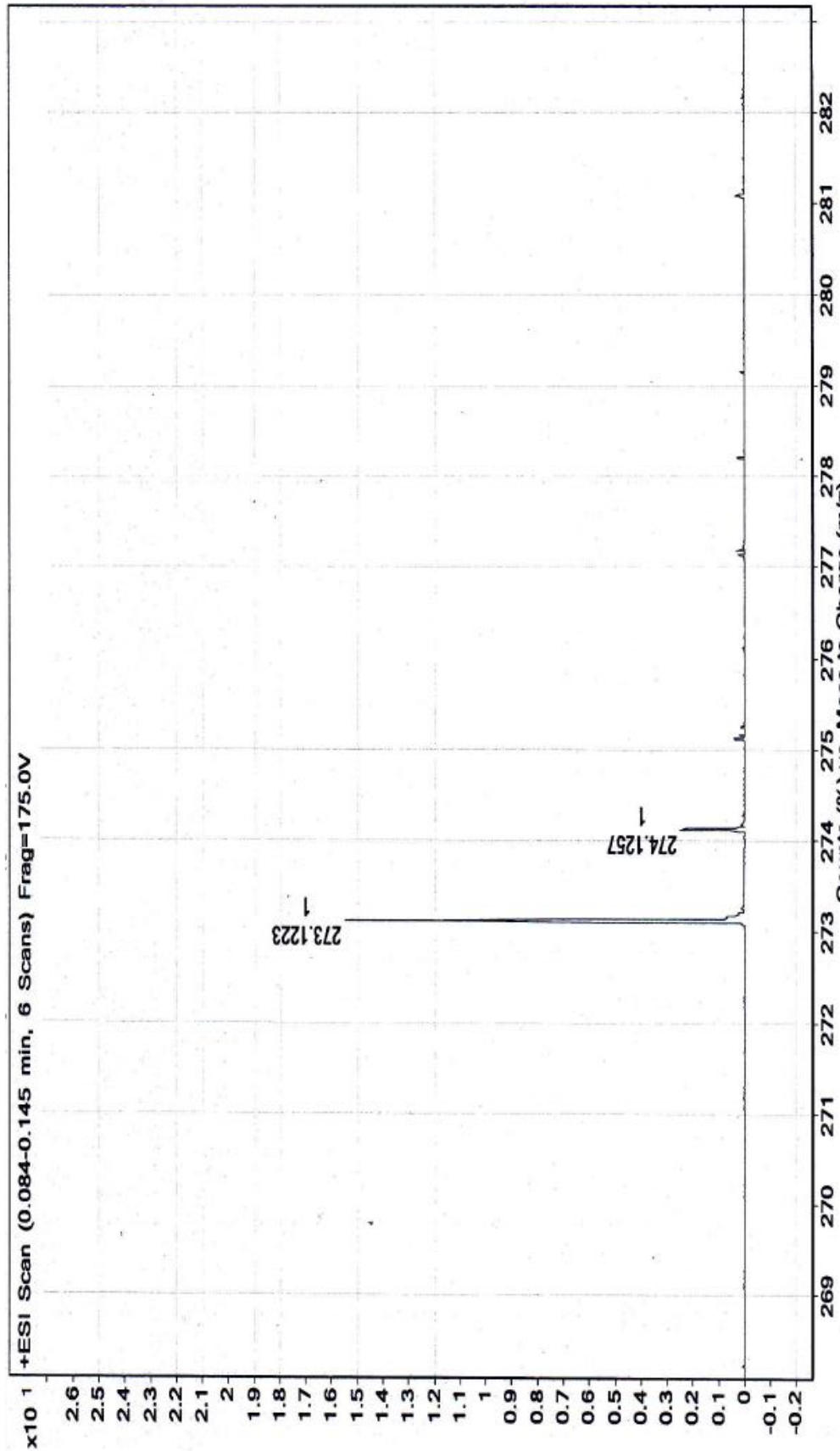


Figure 4.7: MS spectrum of GWS002.

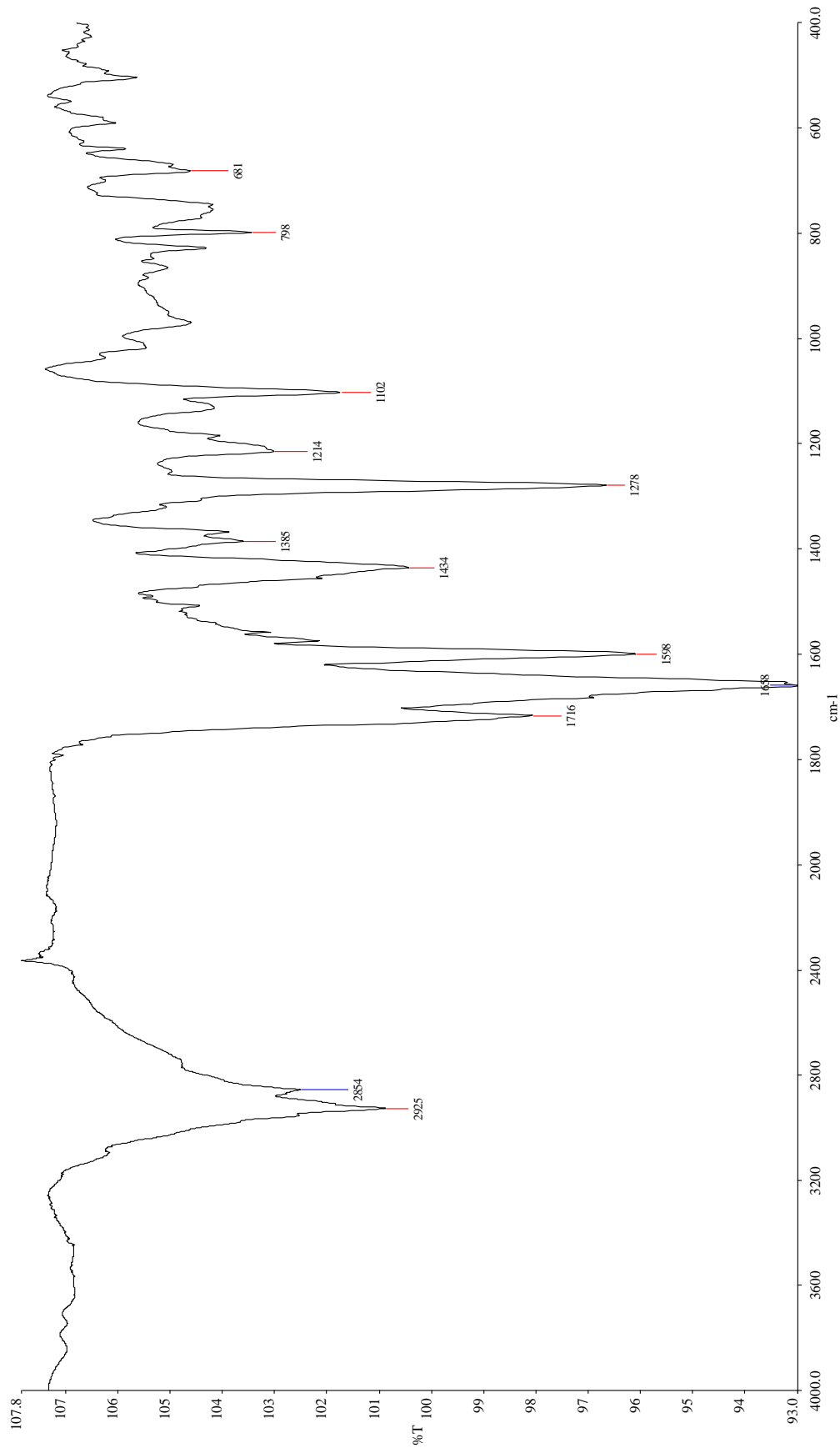


Figure 4.8: FTIR spectrum of GWS002 (thin film on KBr glass).

The proposed structure of **GWS002** is shown in the following figure (Figure 4.9).

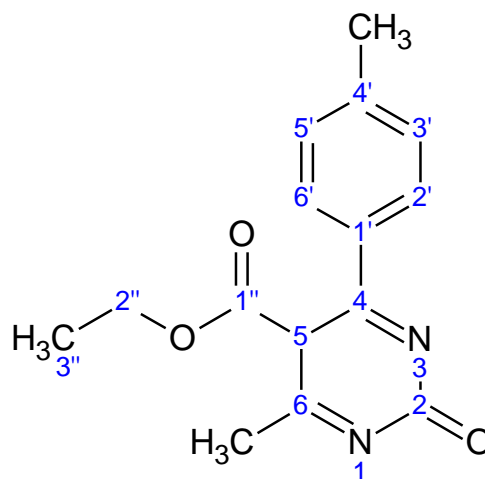


Figure 4.9: Proposed structure of GWS002.

A total of 7 peaks were observed in the ^1H NMR spectrum. A pair of doublet peaks seen at the aromatic region represents the protons at para-substituted aromatic ring. The doublet at δ 7.50 was attributed to the aromatic protons at H-2' and H-6', whereas the peaks at δ 7.23 were assigned to the aromatic protons at H-3' and H-5'. The quartet at δ 4.09 corresponds to the oxy-methylene protons at H-2''. The two signals at δ 2.58 and δ 2.40 were assigned to the protons at 6- CH_3 and 4'- CH_3 , respectively. The singlet peak at δ 1.25 is corresponding to the proton at position H-5. The triplet peaks appeared at δ 0.99 represent the methyl at H-3'' position. In contrast, the two singlet peaks assigned to the protons at N-1 and N-3 position in the ^1H NMR spectrum of **GWS001** no longer exist in the spectrum of **GWS002**. This suggests that the two protons were removed during the electrochemical reaction and confirmed by the molecular formula derived from

HRESIMS. The singlet peak at δ 1.25 was assigned to the proton at position H-4 in **GWS001** was shifted to position H-5 during the reaction.

A total of 11 carbon signals were seen at the ^{13}C NMR spectrum. However, there are actually 15 carbon atoms in the structure of **GWS002**. This is because some of the peaks are overlapping. The DEPT spectrum shows that there are 3 methyl carbons, 1 oxy-methylene carbon, and 3 methine carbons, and 4 quaternary carbons. The taller peak at δ 128.1 is due to the overlapping of signals from two methine groups (C-3' and C-5') and one quaternary carbon (C-1'). The $-\text{CH}_3$ peak at δ 13.5 is taller than the usual $-\text{CH}_3$ peak is because of the overlapping of signals from 2 methyl carbons (C-3'' and 6- CH_3). The signal at δ 1.20 was assigned to the methine carbon at C-5 position. The rest of chemical shifts in the ^{13}C NMR of **GWS002** are comparable with the chemical shifts in that of **GWS001**. The 9 double bond equivalents are contributed by the aromatic ring (4 double bond equivalents), the amide as well as ester group (2 double bond equivalents), the two C=N double bonds (2 double bond equivalents), and the dehydrogenated pyrimidinone ring (1 double bond equivalent).

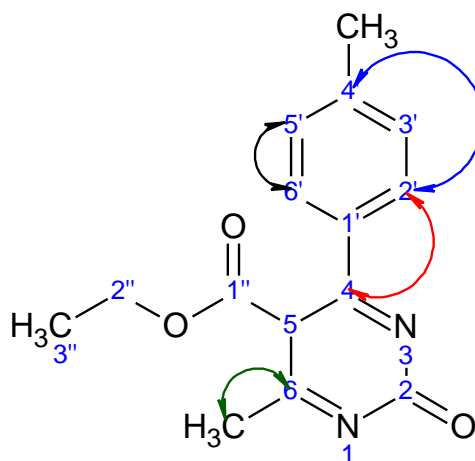


Figure 4.10: Selected HBMC correlations.

A correlation between a carbon and the hydrogen with a distance of either two or three bonds apart will be normally observed in the HMBC spectrum. Based on Figure 4.10 shown above, both the carbons at position C-4 and C-4' showed a three-bond correlation to the protons at position H-2' or H-6' in the spectrum. This suggests that the aryl ring is actually connected to the dehydrogenated pyrimidinone ring. Moreover, the carbon at position C-3' or C-5' also showed correlations to the protons at position H-2' or H-6' with a distance of two-bond apart. Last but not least, a two-bond correlation between the C-6 carbon and the protons at position 6-CH₃ was observed in the HMBC spectrum of **GWS002**. The chemical shifts of each carbon and proton for **GWS002** are listed in the following table (Table 4.8).

Table 4.8: NMR spectra interpretation of GWS002.

Position	δ (ppm), Multiplicity		Coupling Constant, J (Hz)	HMBC
	^{13}C	^1H		
2	158.2, <i>s</i>	—	—	—
4	128.1, <i>s</i>	—	—	H-2' & H-6'
5	1.2, <i>d</i>	1.25, <i>s</i>	—	—
6	111.4, <i>s</i>	—	—	6-CH ₃
6-CH₃	13.5, <i>q</i>	2.58, <i>s</i>	—	—
1'	128.1, <i>s</i>	—	—	—
2' & 6'	129.1, <i>d</i>	7.50, <i>d</i>	8.2	4'-CH ₃ H-3' & H-5'
3' & 5'	128.1, <i>d</i>	7.23, <i>d</i>	8.2	H-2' & H-6'
4'	141.4, <i>s</i>	—	—	4'-CH ₃ H-2' & H-6'
4'-CH₃	21.4, <i>q</i>	2.40, <i>s</i>	—	H-3' & H-5'
1''	166.3, <i>s</i>	—	—	H-2''
2''	61.6, <i>t</i>	4.09, <i>q</i>	7.1	H-3''
3''	13.5, <i>q</i>	0.99, <i>t</i>	7.1	H-2''

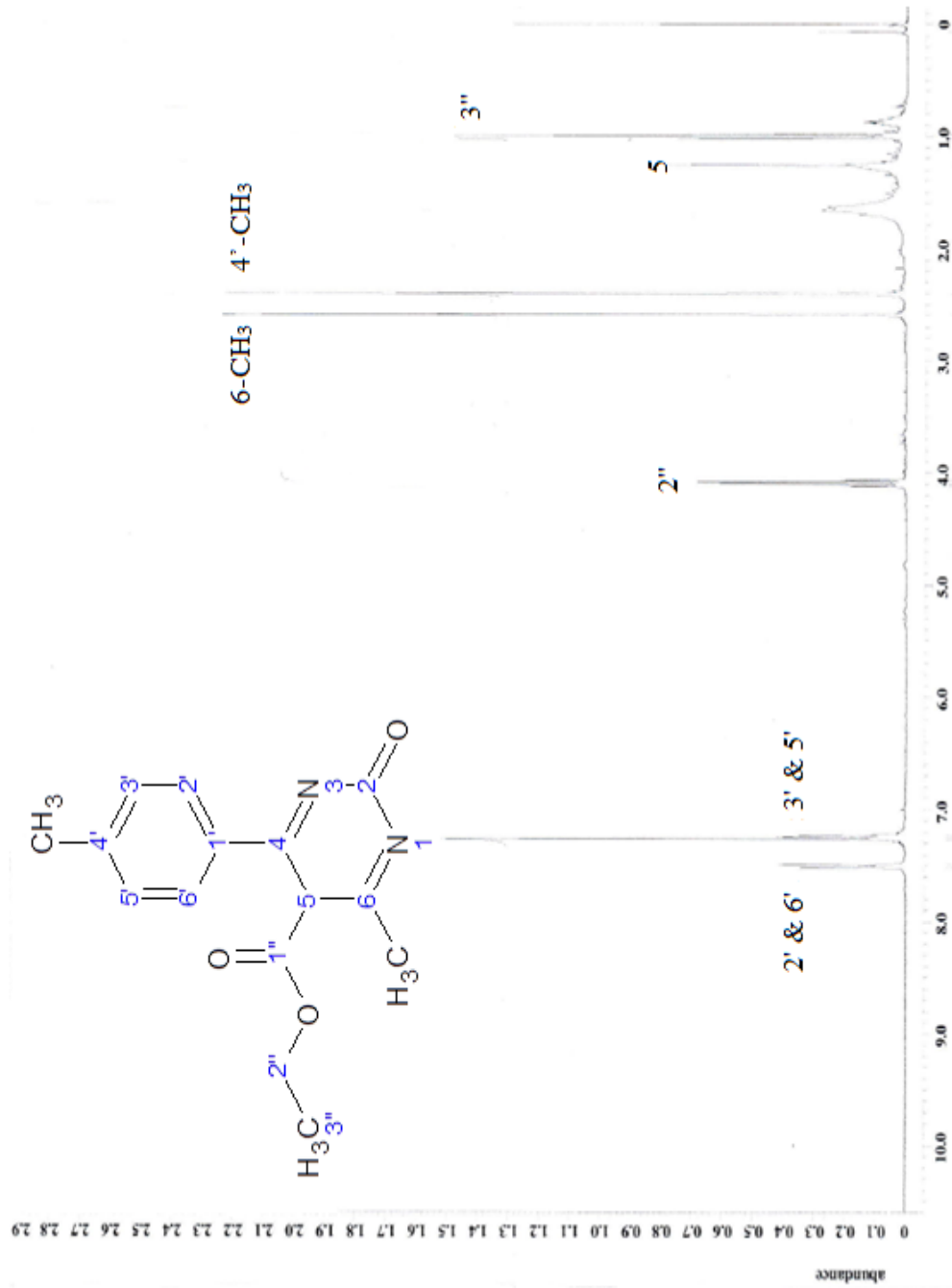


Figure 4.11: ^1H NMR spectrum of GWS002 in CDCl_3 (400 MHz).

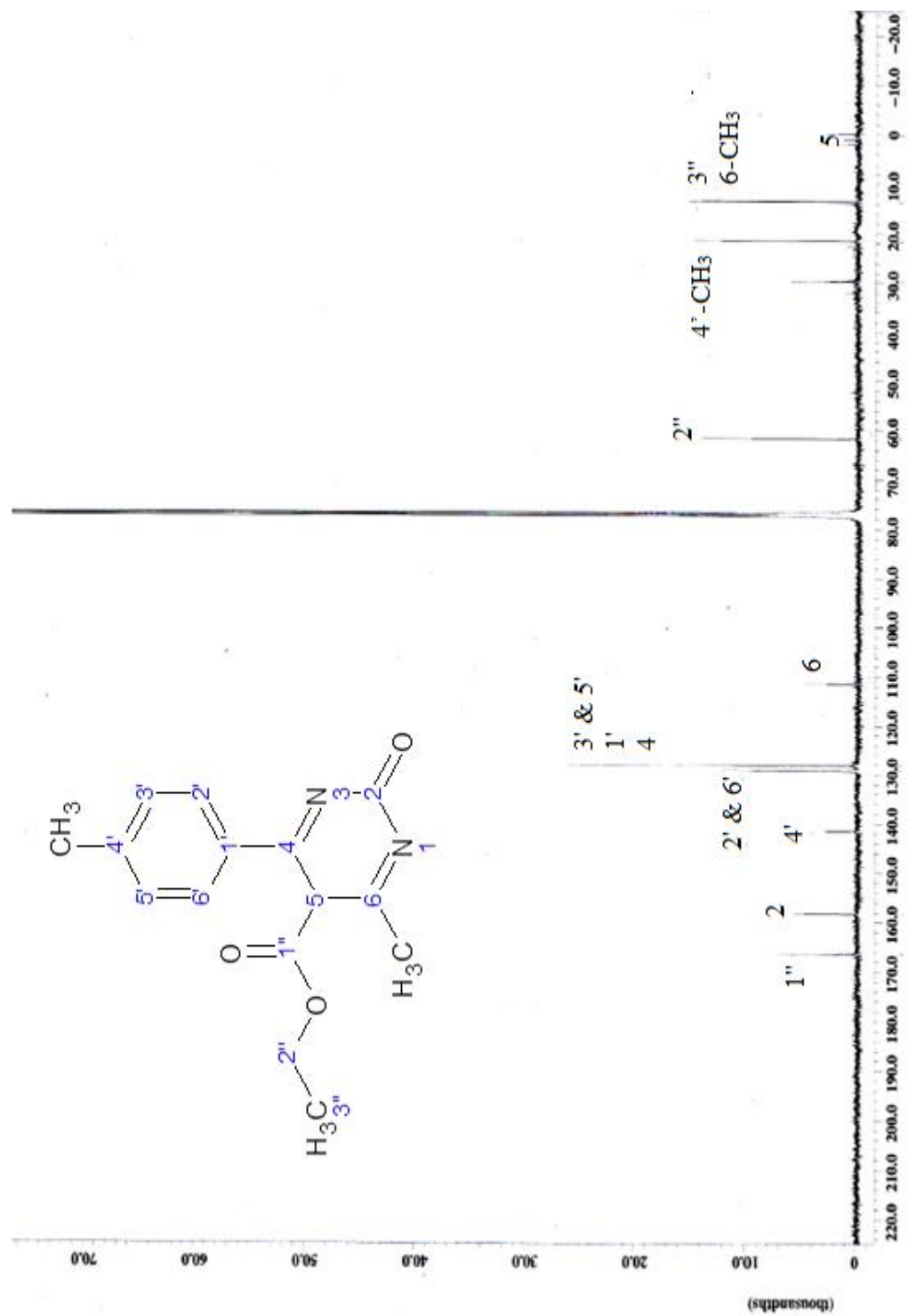
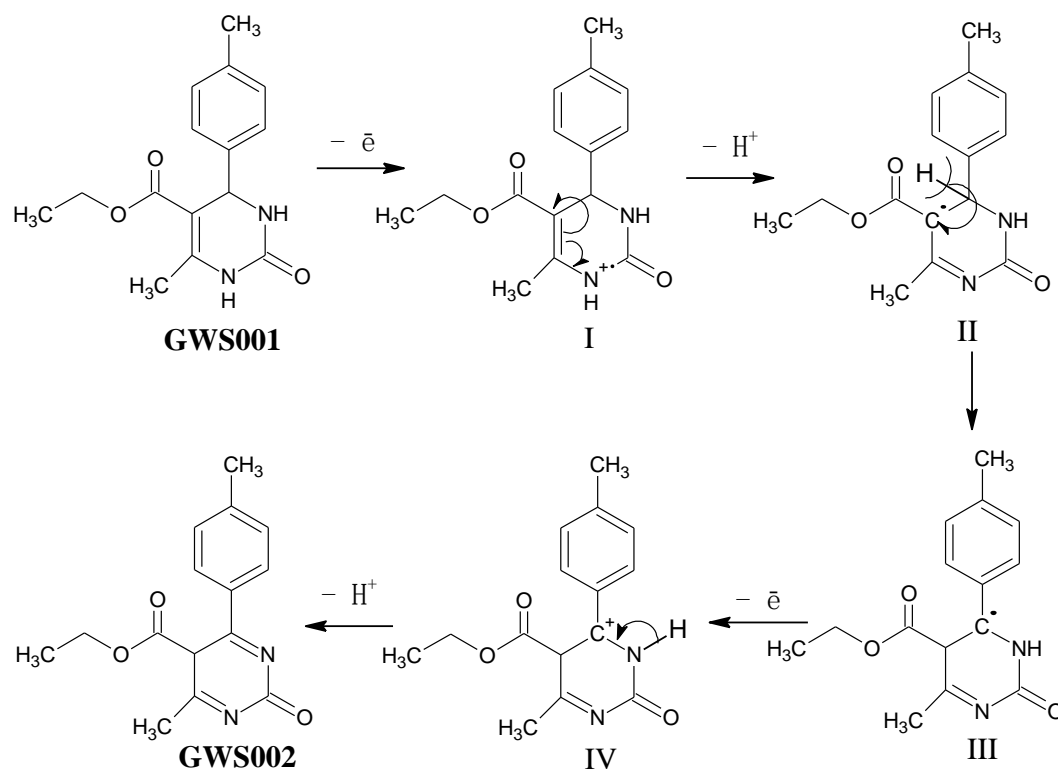


Figure 4.12: ^{13}C NMR spectrum of GWS002 in CDCl_3 (100 MHz).

A mechanism is proposed to explain the formation of **GWS002** from the controlled potential electrolysis. Firstly, one electron is removed from the lone pair of nitrogen atom at N-1 position of the substrate **GWS001** in the electrode process, resulting in the formation of cation radical I (Memarian, et al., 2012). The radical cation then undergoes double bond rearrangement and followed by deprotonation to form the radical II. The intermediate III is resulted from the intramolecular rearrangement of radical II. In the rearrangement, the hydrogen at position H-4 is shifted to the position H-5. After that, the subsequent removal of one electron from carbon at position C-4 of the intermediate III, resulting in the formation of cation IV. The cation then undergoes deprotonation to give the isolated product **GWS002**.



Scheme 4.1: Proposed mechanism for the formation of GWS002.

4.2.2 Electrolysis of 5-Ethoxycarbonyl-6-methyl-4-(*p*-tolyl)-3,4-dihydropyrimidin-2(1*H*)-one in 50% Acetonitrile-Methanol

In the cyclic voltammetric study of **GWS001** in 50% acetonitrile-methanol, the scan was started in the increasing positive potential sweep to be followed by the scan in opposite direction with a decrease in potential. By comparing with the cyclic voltammogram of the blank, an additional oxidation peak was observed at a potential of 1.41 V as shown in the voltammogram (Figure 4.13) With the subsequent addition of potassium hydroxide, the peak was enhanced and shifted to a lower potential of 1.23 V. This suggests that that the reaction involves the release of protons.

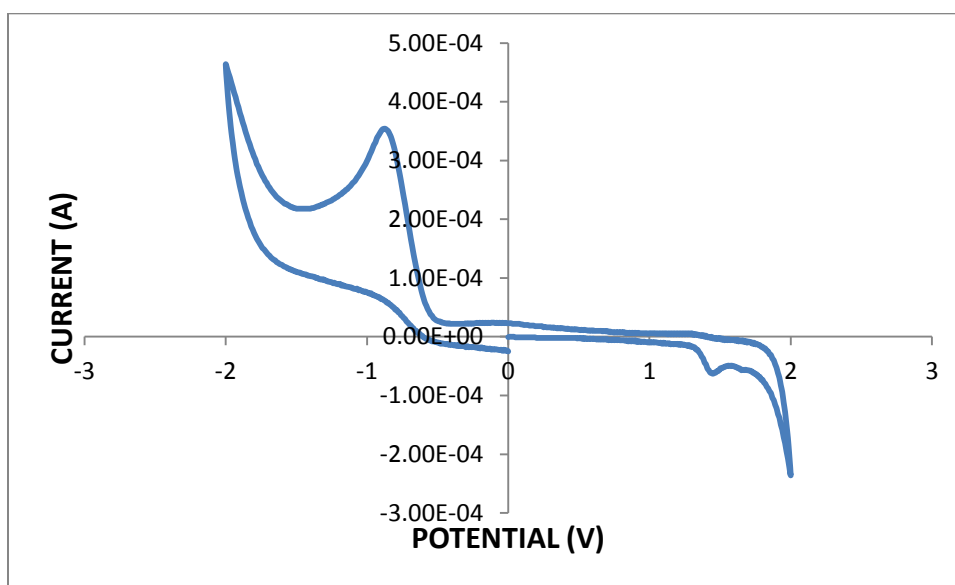


Figure 4.13: Cyclic voltammogram of GWS001 (5 mg) at glassy carbon rod working electrode, platinum coil wire counter electrode, and silver-silver chloride reference electrode in 50% acetonitrile-methanol.

In the controlled potential electrolysis, the potential was set a little higher than the oxidation potential peak resulted from the addition of potassium hydroxide. This was to make sure that the substrate was fully consumed. The time required for the electrolysis of **GWS001** in solvent composition of 50% acetonitrile with 50% methanol was 15840 seconds. A total of 13 electrons transferred per substrate molecule were calculated by applying Faraday's law. The total isolated weight of was 18.4 mg; however the weight of interest product, **GWS003** was only 4.1 mg with yield 12%.

GWS003 was obtained as a solid after the electrolysis. The retardation factor (R_f) of **GWS003** in the solvent system chloroform: acetonitrile (4: 1) was obtained as 0.44. HRESIMS gave a pseudo molecular ion at 331.1275 $[M+Na]^+$ for a molecular formula $C_{15}H_{20}N_2O_5$. The molecular formula shows that there is an increase of two hydrogen and two oxygen atoms while the double bond equivalent has decreased one to seven. The molecular formula and its corresponding molecular ion as well as double equivalent are listed in the following table (Table 4.9).

Table 4.9: Molecular formula and its respective molecular ion as well as double bond equivalent of GWS003 provided by HRESIMS.

Molecular Formula of GWS003	Molecular Ion $[M+Na]^+$		Double Bond Equivalent
	Observed	Calculated	
$C_{15}H_{20}N_2O_5$	331.1275	331.1274	7

In the FTIR spectrum of **GWS003**, the absorption of N-H stretch was detected at wavenumber of 3289 cm^{-1} . The absorption peaks at wavenumber of 3103 cm^{-1} and 2948 cm^{-1} are due to the aromatic C-H stretch and the sp^3 C-H stretch, respectively. Other than that, the spectrum shows the strong absorption peak at wavenumber at 1692 cm^{-1} indicating the C=O stretch. A pair of absorptions at wavenumbers of 1680 cm^{-1} and 1437 cm^{-1} represents the aromatic C=C stretch. The two medium absorption peaks at wavenumber of 1326 cm^{-1} and 1090 cm^{-1} indicate the C-O stretch and C-N stretch, respectively. The wavenumbers and their corresponding vibration mode for the various functional groups of **GWS003** are listed in the following table (Table 4.10).

Table 4.10: FTIR spectrum interpretation of GWS003.

Wavenumber (cm^{-1})	Vibration Mode
3289	N-H stretch
3103	Aromatic C-H stretch
2948	sp^3 C-H stretch
1692	C=O stretch
1680 & 1437	Aromatic C=C stretch
1326	C-O stretch
1090	C-N stretch

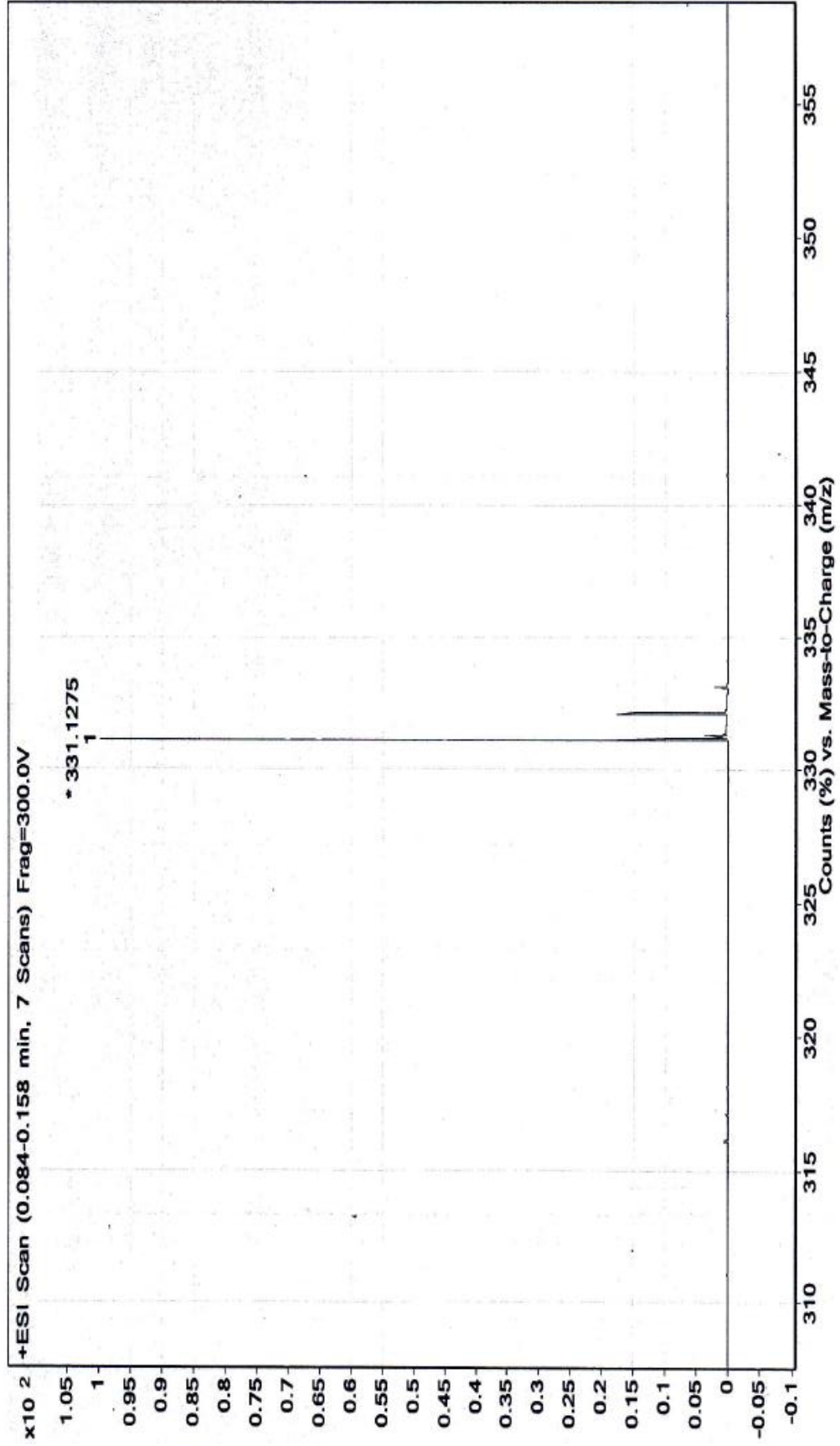


Figure 4.14: MS spectrum of GWS003.

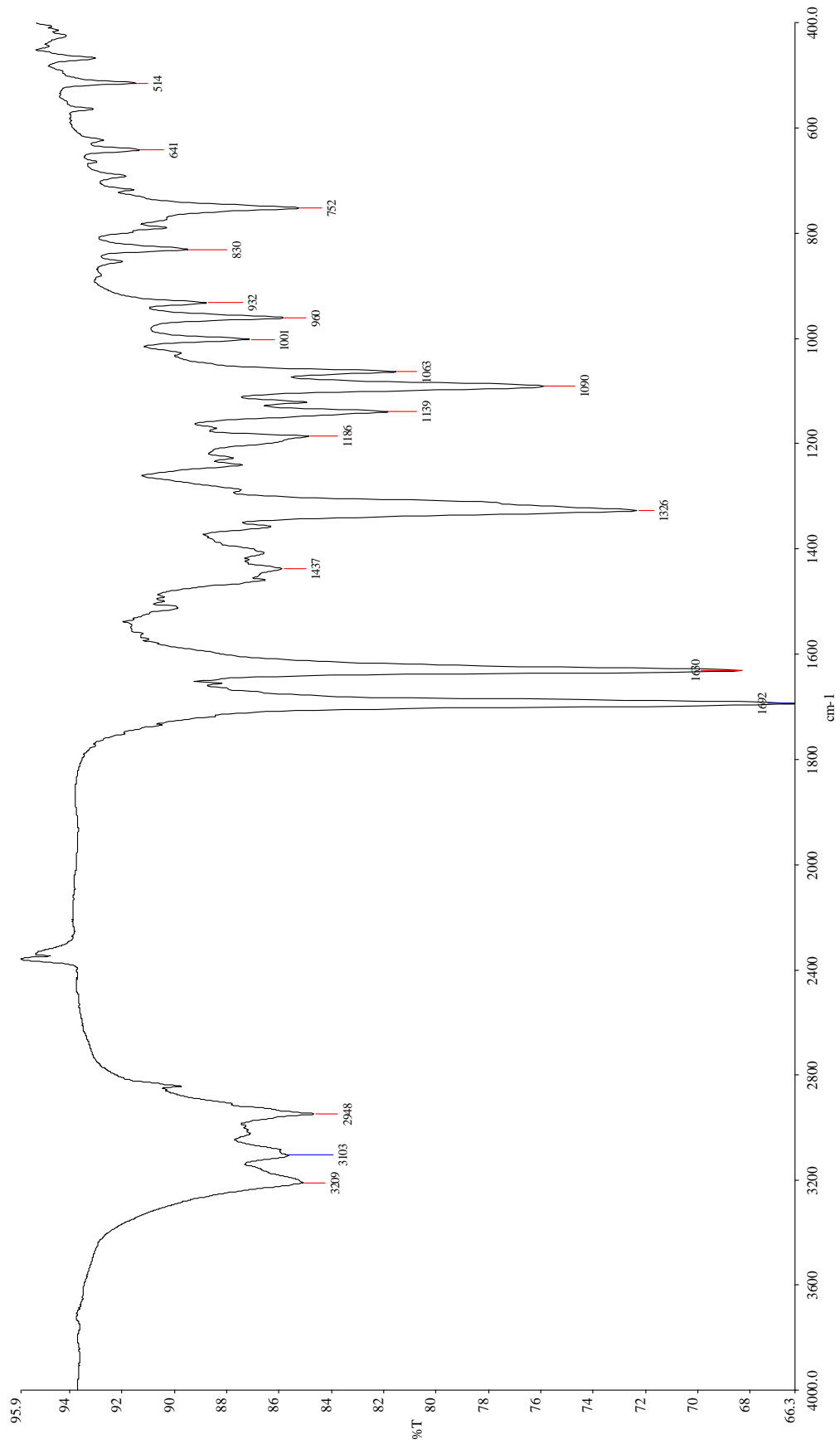


Figure 4.15: FTIR spectrum of GWS003 (thin film on KBr glass).

A proposed structure of **GWS003** is shown Figure 4.16 below.

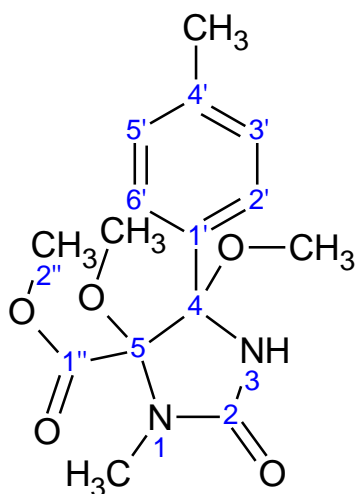


Figure 4.16: Proposed structure of GWS003.

A total of 8 peaks were observed in the ^1H NMR spectrum. A pair of doublet peaks shown at the low field region indicates the protons at para-substituted aromatic ring. The doublet peaks at δ 7.50 were attributed to the aromatic protons at H-2' and H-6', while the peaks at δ 7.25 were assigned to the aromatic protons at H-3' and H-5'. The singlet peaks at δ 5.94 was assigned to H-3. The singlet at δ 4.05 corresponds to the methoxy protons at H-2''. The three singlet peaks observed at δ 3.27, δ 3.23, δ 2.99 are corresponding to the protons at 1-CH₃ and 4-OCH₃, and 5-OCH₃ respectively. Lastly, the singlet peak appeared at δ 1.61 was assigned to the protons at 4'-CH₃ position.

A total of 13 carbon signals were seen at the ^{13}C NMR. However, there are actually 15 carbon atoms present in **GWS003**. This could be due to some of the peaks are overlapping. The DEPT spectrum shows that there are 5 methyl carbons

and 2 methine carbons, and 6 quaternary carbons. The 2 peaks in the low field region at δ 173.7 and δ 157.4 are corresponding to the ester group carbon at position C-1'' and the amide group carbon at position C-2, respectively. The ester and amide group contribute to 2 double bond equivalents.

The two signals at δ 139.7 and δ 130.4 were assigned to the carbons at position C-4' and C-1' respectively. The two peaks at δ 129.2 and δ 128.6 represent the methine carbons at the aromatic ring. The peak at δ 129.2 was assigned to the aromatic ring carbons at position C-2' and C-6', but the signal at δ 128.6 was assigned to the carbons at position C-3' and C-5'. This aromatic ring contributes to 4 double bond equivalents. The last double bond equivalent left is due to the imidazolidinone ring. The two signals at δ 96.7 and δ 89.4.2 indicate the quaternary carbons at position C-5 and C-4 respectively. They both are attached to two electronegative atoms, oxygen and nitrogen making them more deshielded.

The series of peaks at δ 55.7, δ 52.0, and δ 50.3 are resonances from the methoxy carbons at C-2'', 5-OCH₃, and 4-OCH₃. The signal at δ 53.2 is due to the methyl carbon attached to the nitrogen at position N-1. The last peak at δ 21.1 was assigned to the carbon at position C-4'.

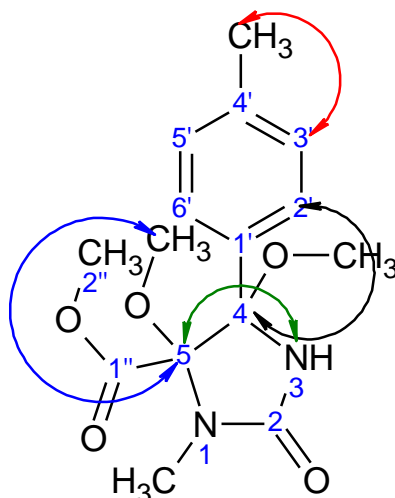


Figure 4.17: Selected HMBC correlations.

Based on the HMBC correlations shown in Figure 4.17, the carbon at position 4'-CH₃ showed a correlation to the proton at position H-3' or H-5' with a distance of three bonds apart. Moreover, a three-bond correlation between the carbon at position C-4 and the proton at position H-2' was observed in the HMBC. This shows the connection between the para-substituted aromatic ring and the imidazolidinone ring. The carbon at position C-5 showed a three-bond correlation with proton at position N-3. Besides that, the carbons also correlated to the proton at position 5-OCH₃ with a distance of three bonds apart. The chemical shifts of each carbon and proton for **GWS003** are listed in the following table (Table 4.11).

Table 4.11: NMR spectra interpretation of GWS003.

Position	δ (ppm), Multiplicity		Coupling Constant, J (Hz)	HMBC
	^{13}C	^1H		
1-CH ₃	53.2, <i>q</i>	3.27, <i>s</i>	—	—
2	157.4, <i>s</i>	—	—	—
3	—	5.94, <i>s</i>	—	—
4	89.4, <i>s</i>	—	—	4-OCH ₃ N-3
4-OCH ₃	50.3, <i>q</i>	3.23, <i>s</i>	—	—
5	96.7, <i>s</i>	—	—	5-OCH ₃ 1-CH ₃ N-3
5-OCH ₃	52.0, <i>q</i>	2.99, <i>s</i>	—	—
1'	130.4, <i>s</i>	—	—	H-3' & H-5'
2' & 6'	129.2, <i>d</i>	7.50, <i>d</i>	8.2	—
3' & 5'	128.6, <i>d</i>	7.25, <i>d</i>	8.2	4'-CH ₃ H-2' & H-6'
4'	139.7, <i>s</i>	—	—	4'-CH ₃ H-2' & H-6'
4'-CH ₃	21.1, <i>q</i>	2.38, <i>s</i>	—	H-3' & H-5'
1''	173.7, <i>s</i>	—	—	H-2''
2''	55.7, <i>q</i>	4.05, <i>s</i>	—	—

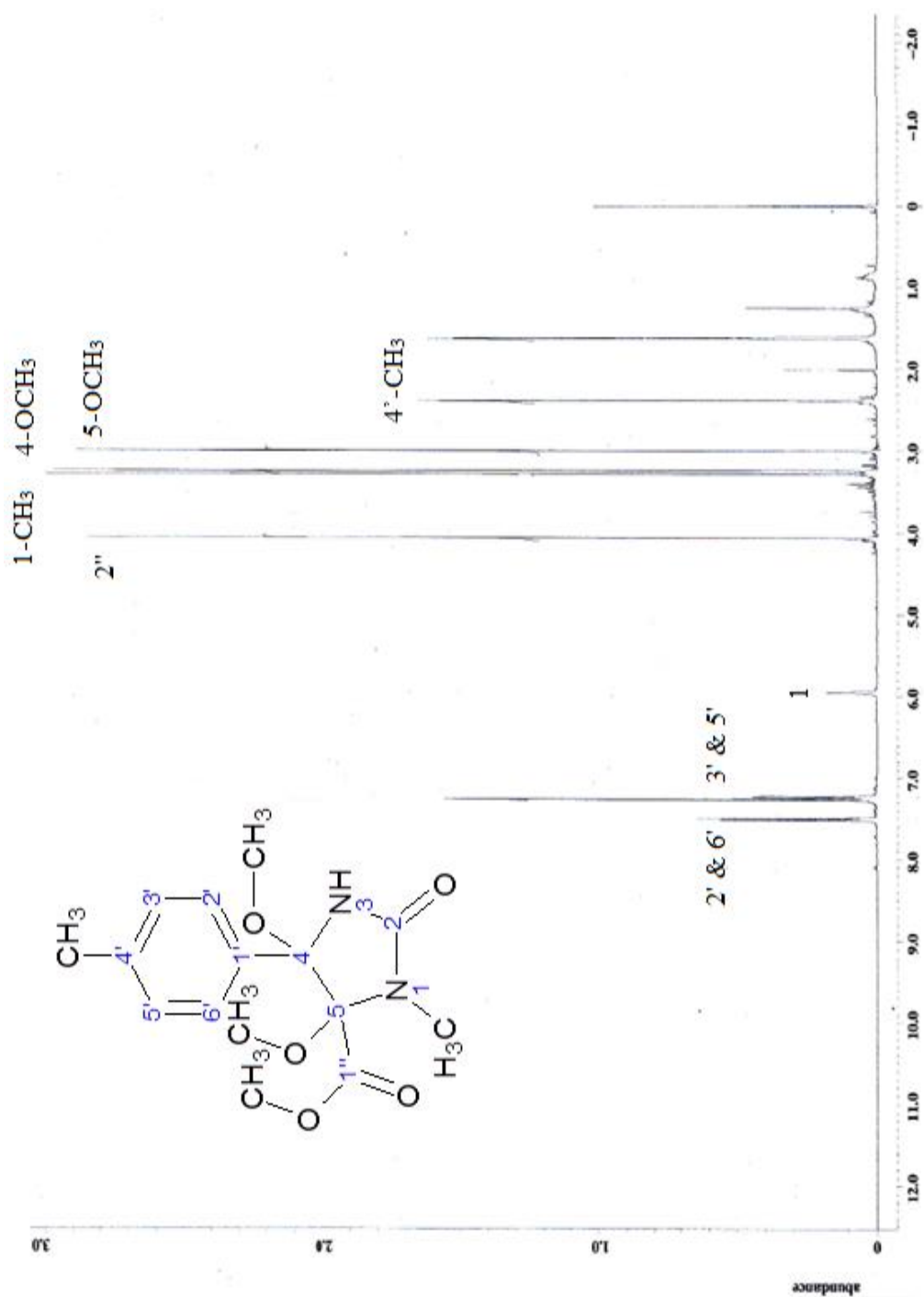


Figure 4.18: ¹H NMR spectrum of GWS003 in CDCl₃ (400 MHz).

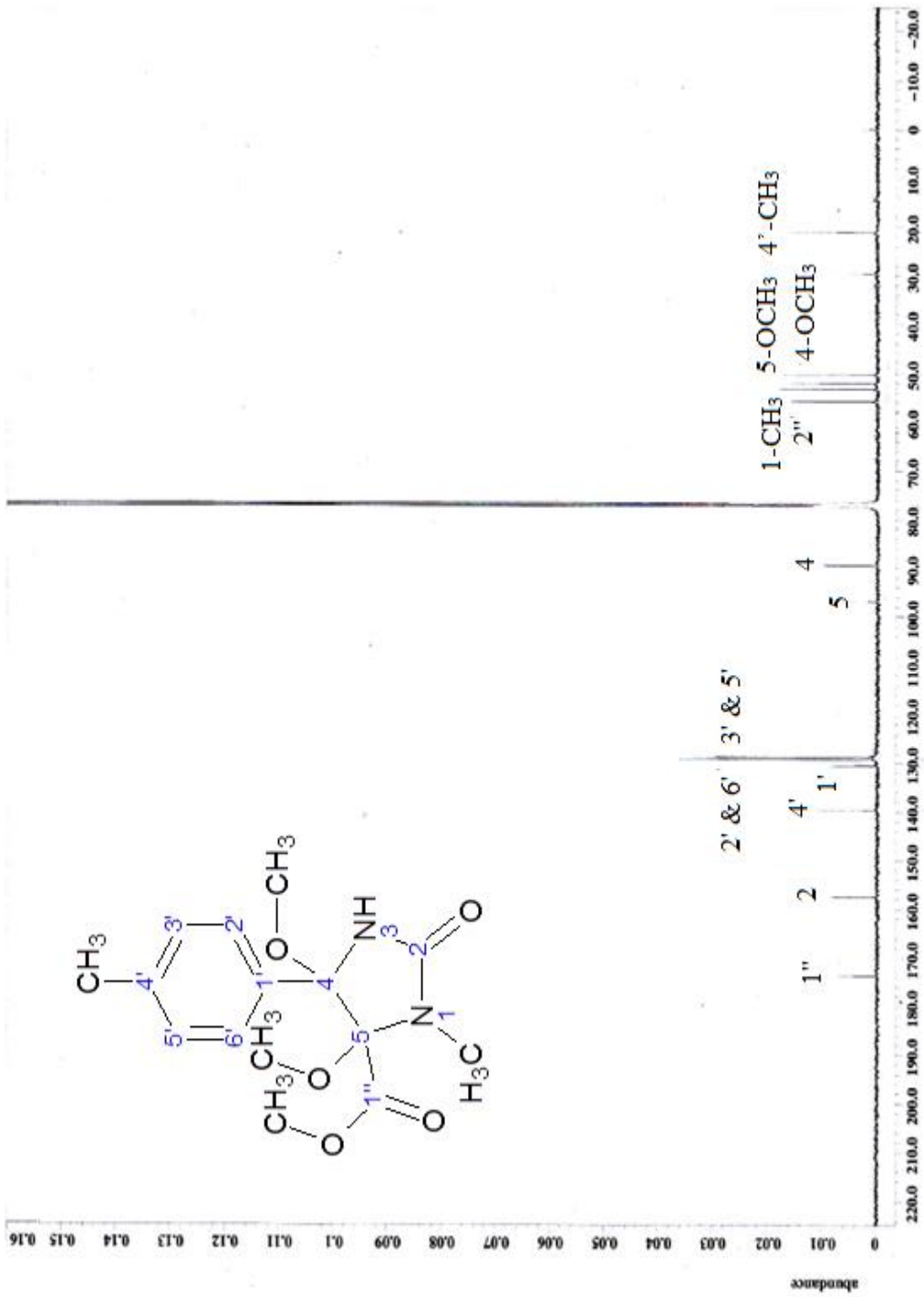


Figure 4.19: ^{13}C NMR spectrum of GWS003 in CDCl_3 (100 MHz).

4.2.2 Electrolysis of 5-Ethoxycarbonyl-6-methyl-4-(*p*-tolyl)-3,4-dihydropyrimidin-2(1*H*)-one in 50% Acetonitrile-Acetone

When cyclic voltammetric study of **GWS001** was repeated in 50% acetonitrile-acetone, an oxidation peak was observed at 1.56 V was shown in the voltammogram below (Figure 4.20). With subsequent addition of potassium hydroxide, the peak was enhanced and shifted to a smaller potential of 1.18 V.

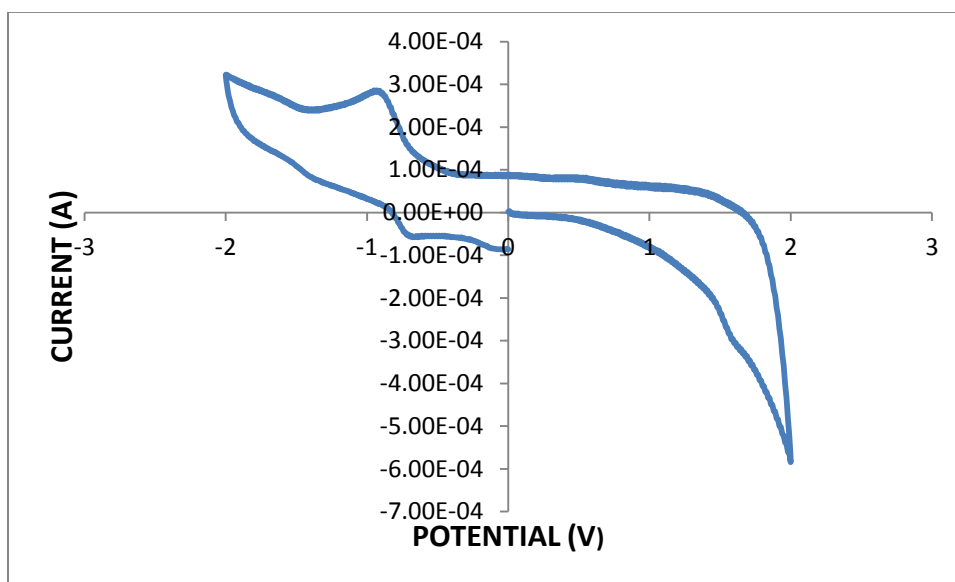


Figure 4.20: Cyclic voltammogram of GWS001 (5 mg) at glassy carbon rod working electrode, isolated platinum coil wire counter electrode, and silver-silver chloride reference electrode in 50% acetonitrile-acetone.

The reaction was stopped after 10080 seconds when the current achieved a constant value. Based on the calculation using Faraday's law, a total of 5 electrons transferred per substrate molecule was obtained. The total crude yield was 16.2 mg; however the weight of interest product, **GWS004** was only 5.3 mg with yield of 19%. **GWS004** was obtained as a solid after the electrolysis. The

retardation factor (R_f) of **GWS004** in the solvent system chloroform: acetonitrile (4: 1) was obtained as 0.25.

In the FTIR spectrum of **GWS004**, the absorption of N-H stretch was detected at wavenumber of 3387 cm^{-1} . The aromatic C-H stretch and the sp^3 C-H stretch were detected at wavenumber of 3175 cm^{-1} and 2972 cm^{-1} , respectively. The spectrum shows a strong absorption peak at wavenumber at 1644 cm^{-1} indicating a conjugated ketone C=O stretch. A pair of absorptions at wavenumbers of 1614 cm^{-1} and 1410 cm^{-1} are due to the aromatic C=C stretch. The wavenumbers and its corresponding vibration mode for the various functional groups of **GWS004** are listed in the following table (Table 4.12).

Table 4.12: FTIR spectrum interpretation of GWS004.

Wavenumber (cm^{-1})	Vibration Mode
3387	N-H stretch
3175	Aromatic C-H stretch
2972	sp^3 C-H stretch
1644	Ketone C=O stretch
1614 & 1410	Aromatic C=C stretch

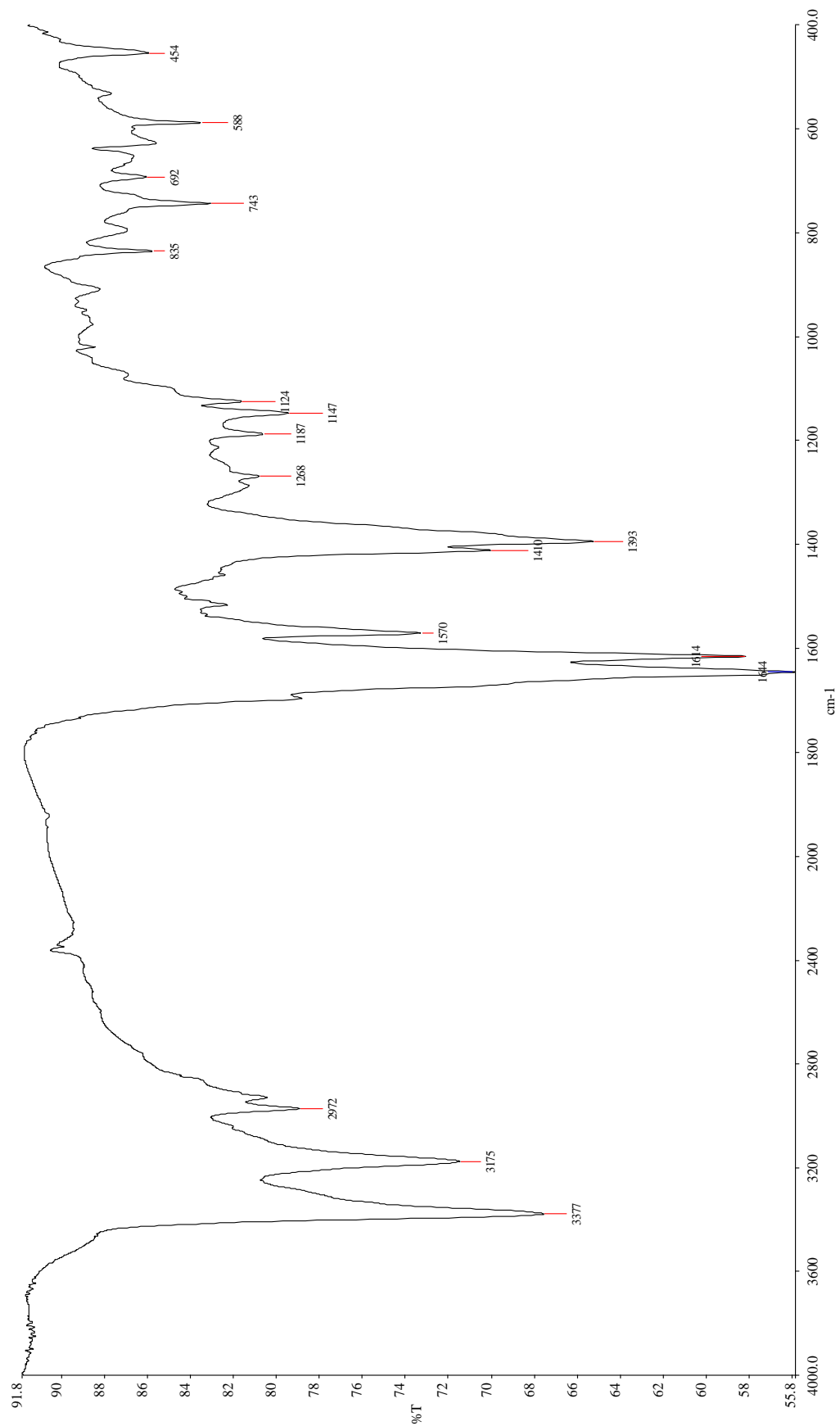


Figure 4.21: FTIR spectrum of GWS004 (thin film on KBr glass).

A proposed structure of **GWS004** is shown in Figure 4.22 below.

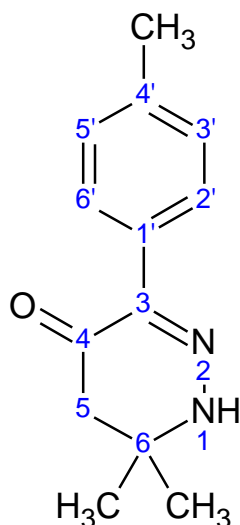


Figure 4.22: Proposed structure of GWS004.

A total of 6 peaks were seen in the ^1H NMR spectrum. A pair of doublet peaks shown at the aromatic region indicates the protons at aryl ring. The doublet at δ 7.71 was assigned to the protons at H-2' and H-6', whereas the peaks at δ 7.26 were assigned to the aromatic protons at H-3' and H-5'. The singlet peak at δ 3.56 was assigned to the proton at position H-1. The singlet signal at δ 2.63 is corresponding to the protons at position H-5. While the singlet observed at δ 2.40 was assigned to the protons at 4'-CH₃. Lastly, the peak appeared at δ 1.29 is due to the signal overlapping from protons at position at 6-CH₃.

A total of 10 carbon signals were seen at the ^{13}C NMR. However, there are actually 13 carbon atoms present in **GWS004**. This could be due to some of the peaks are overlapping. The DEPT spectrum shows that there are 2 methyl carbons,

1 methylene carbon and 2 methine carbons, and 5 quaternary carbons. The peak in the low field region at δ 214.6 was assigned to the ketone group carbon at position C-4. The peak at δ 169.6 was assigned to the imine carbon at position C-3. The signals at δ 142.7 and δ 130.6 indicate the carbons at position C-1' and C-4' respectively. The two peaks at δ 129.4 and δ 127.5 represent the methine carbons on the aryl ring. The peak at δ 129.4 was assigned to the aromatic ring carbons at position C-3' and C-5', while the signal at δ 127.5 was assigned to the carbons at position C-2' and C-6'. The signal at δ 69.9 is corresponding to the quaternary carbons at position C-6. The methylene carbon at position C-5 has a shift of δ 55.08. Carbon at C-6 is directly attached to the electronegative nitrogen atom making it more deshielded.

The two signals in the high field region at δ 29.5 and 21.6 are due to the methyl carbons at position 1''-CH₃ and 4'-CH₃, respectively. One of the -CH₃ peaks appeared to be taller than the normal CH₃ and this could be due to the overlapping of signals from the two methyl groups at position C-6.

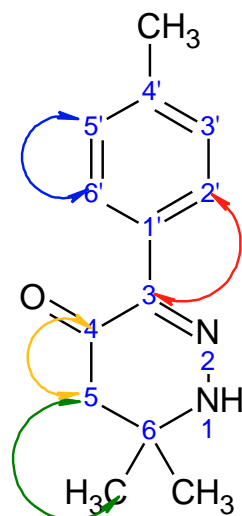


Figure 4.23: Selected HMBC correlations.

Based on Figure 4.23 shown as above, the carbon at position C-3 showed a three-bond correlation to the proton at position H-2' or H-6'. This suggests that the aryl ring is actually connected to the pyridazin-4(1*H*)-one ring. Moreover, the carbon at position C-3' or C-5' also correlated to the proton at position H-2' or H-6' with a distance of two-bond apart. A two-bond correlation between the C-4 carbon and the protons at position C-5 was observed in the HMBC spectrum of **GWS004**. Besides that, the methyl carbons at position 6-CH₃ also correlated to the C-5 protons with a distance of three-bond apart. The chemical shifts of each carbon and proton for **GWS004** are listed in the following table (Table 4.13). However, the proposed structure could not be confirmed without MS data.

Table 4.13: NMR spectra interpretation of GWS004.

Position	δ (ppm), Multiplicity		Coupling Constant, J (Hz)	HMBC
	^{13}C	^1H		
1	—	3.56, <i>s</i>	—	—
3	169.6, <i>s</i>	—	—	H-2' & H-6'
4	214.6, <i>s</i>	—	—	H-5
5	55.0, <i>t</i>	2.63, <i>s</i>	—	6-CH ₃
6	69.9, <i>s</i>	—	—	6-CH ₃ H-5
6-CH₃	29.5, <i>q</i>	1.29, <i>s</i>	—	6-CH ₃ H-5
1'	130.6, <i>s</i>	—	—	H-2' & H-6'
2' & 6'	129.4, <i>d</i>	7.71, <i>d</i>	8.2	4'-CH ₃ H-3' & H-5'
3' & 5'	127.5, <i>d</i>	7.26, <i>d</i>	8.2	H-2' & H-6'
4'	142.7, <i>s</i>	—	—	4'-CH ₃ H-2' & H-6'
4'-CH₃	21.6, <i>q</i>	2.40, <i>s</i>	—	H-3' & H-5'

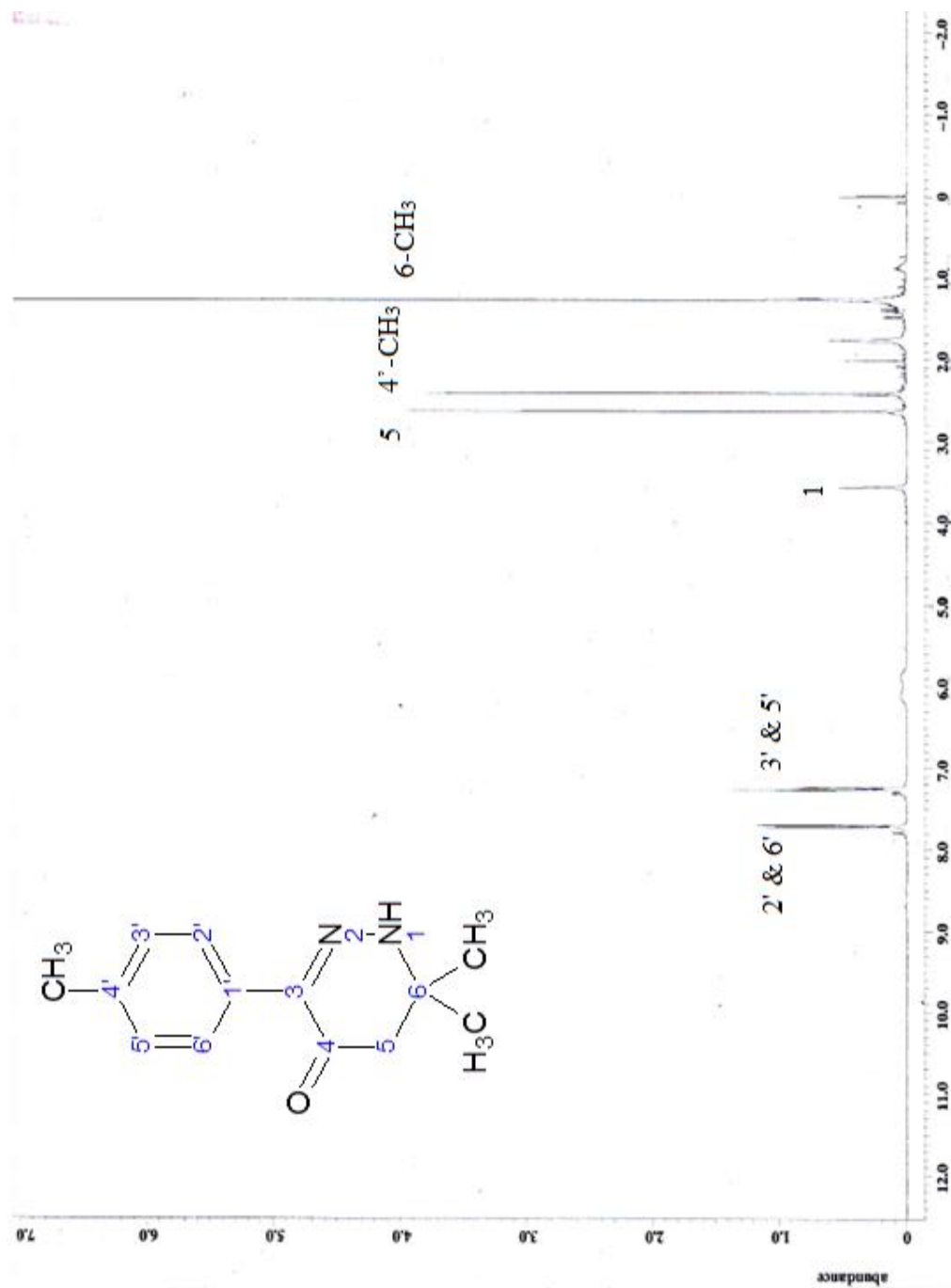


Figure 4.24: ^1H NMR spectrum of GWS004 in CDCl_3 (400 MHz).

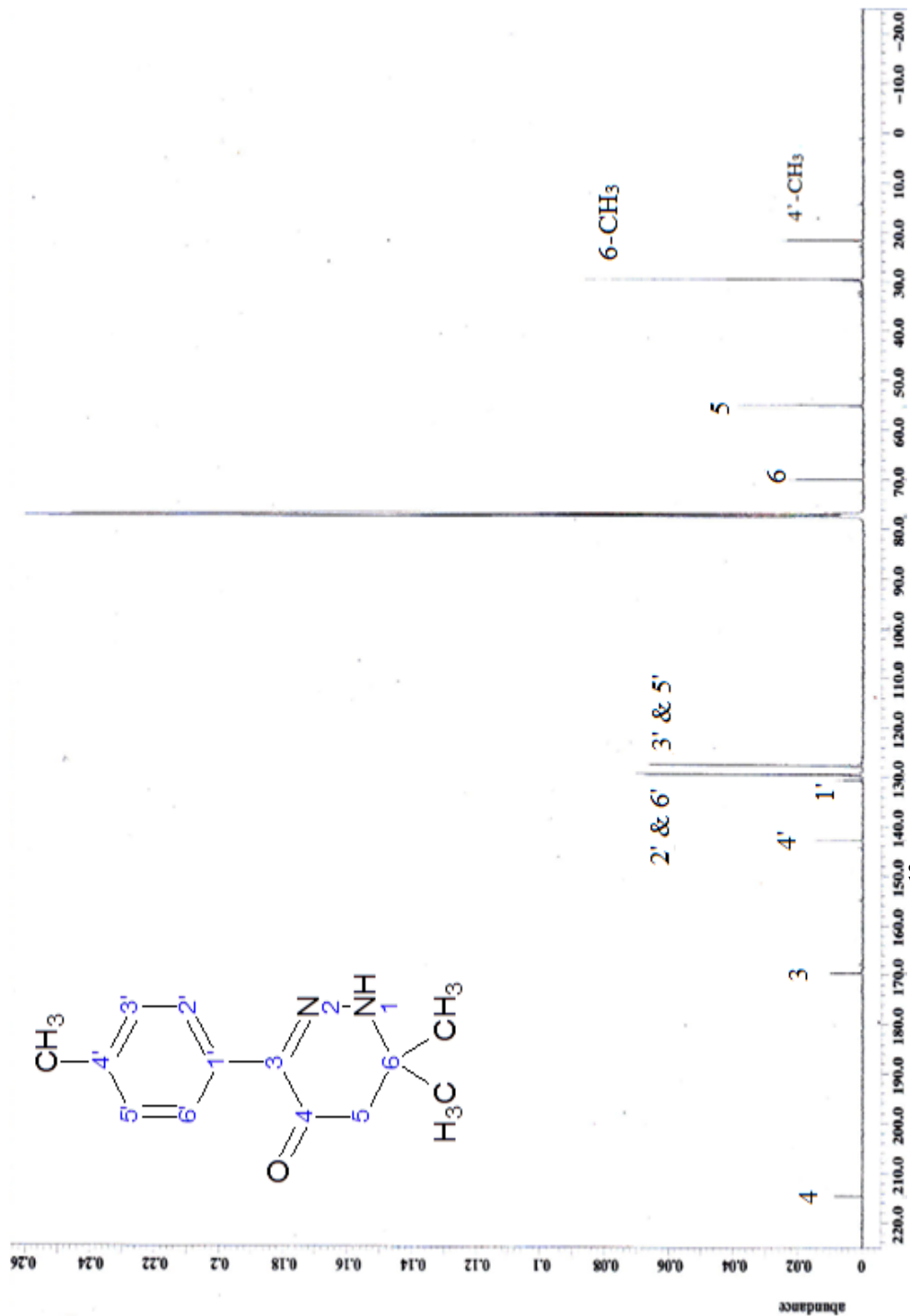


Figure 4.25: ^{13}C NMR spectrum of GWS004 in CDCl_3 (100 MHz).

CHAPTER 5

CONCLUSION AND FURTHER STUDIES

Generally, the electrochemical reactions of 5-ethoxycarbonyl-6-methyl-4-(*p*-tolyl)-3,4-dihydropyrimidin-2(1*H*)-one occurred at the pyrimidinone ring. This statement has been shown by the structures proposed for the electrolysis products. However, the mechanism proposed for the electrochemical reactions of the 3,4-dihydropyrimidin-2(1*H*)-one have to be further confirmed by using trapping agent. The trapping agent is used to react with the intermediate that formed in the electrochemical reactions. As a result, the sequence of reacting site which occurred throughout the electrochemical reaction can be known. By altering other parameters, such as the nature of the electrode material or the supporting electrolyte, different products might be formed during the controlled potential electrolysis (Kam, Lim and Tan, 1999). This provides a useful information in understanding of the electrochemical behavior of the 3,4-dihydropyrimidin-2(1*H*)-one. Furthermore, the reasons that the electrochemical method produced low yield of interest products should be further identified. Last but not least, future studies on the electrochemical reduction of 3,4-dihydropyrimidin-2(1*H*)-one can be considered since the nitrogen atom of the 3,4-dihydropyrimidin-2(1*H*)-one is suspected able to receive electrons from the cathode.

REFERENCES

Aceves, J.M., Miranda, R. and Kappe, C.O. 2007. Electrooxidation of Biginelli dihydropyrimidones. *ECS Transactions*, 3(32), pp. 41-55.

Ebersson, L. and Schäfer, H., 1971. *Organic electrochemistry*. Berlin Heidelberg: Springer.

Goyal, R.N., Klumar, A., Jain, N. and Gupta, P., 1999. Electrochemical oxidation of 6-hydroxy-2,4,5-triaminopyrimidine at pyrolytic graphite electrode. *Indian Journal of Chemistry*, 38A(10), pp. 1015-1023.

Hayes, B.L., 2002. *Microwave synthesis: chemistry at the speed of light*. Matthews: CEM Publishing.

Kadysh, V., Stradins, J. Khanina, H. and Duburs, G., 1989. Electrochemical oxidation of 4-aryl-1,4-dihydropyrimidines on a carbon electrode. *Electrochimica Acta*, 34(7), pp. 899-904.

Kam, T.S., Lim, T.M. and Tan, G.H., 1999. Anodic oxidation of the aspidofractinine alkaloid kopsamine. *Heterocycles*, 51(2), 249-253.

Lawrence, S.A., 2004. *Amines: synthesis, properties, and applications*. Cambridge: Cambridge University Press.

Lee, M.K., 2012. *Electrochemical behavior of the 4,6-diphenylpyrimidin-2(1H)-one*. B.Sc. Universiti Tunku Abdul Rahman.

Ludvík, J., Volke, J. and Klíma, J., 1987. Electrochemical oxidation of different type 1, 4-dihydropyridine derivatives in acetonitrile. *Electrochimica Acta*, 32(7), pp. 1063-1071.

Lund, H. and Hammerich, O. eds., 2001. *Organic electrochemistry*. 4th ed. New York: Marcel Dekker.

Maskill, H. ed., 2006. *The investigation of organic reactions and their mechanisms*. Oxford: Blackwell Publishing.

Memarian, H.R., Soleymani, M., Sabzyan, H., Bagherzadeh, M. and Ahmadi, H., 2011. Voltammetric oxidation of 2-oxo-1,2,3,4-tetrahydropyrimidin-5-carboxamides: substituent effects. *Journal of Physical Chemistry A*, 115(29), pp. 8264-8270.

Memarian, H.R., Ranjbar M., Sabzyan, H., Kiani, A., 2012. Substituent effects on the voltammetric studies of 2-oxo-1,2,3,4-tetrahydropyrimidines, *Comptes Rendus Chimie*, 15(11-12), pp. 1001-1011.

Mirza-Aghayan, M., Bolourtchian, M. and Hosseini, M., 2004. Microwave-assisted efficient synthesis of dihydropyrimidines in solvent-free condition. *Synthetic Communications*, 34(18), pp. 3335-3341.

Núñez-Vergara L.J., Sturm, J.C., Alvarez-Lueje A., Olea-Azar, C., Sunkel, C. and Squella, J.A. 1999. Electrochemical oxidation of 4-methyl-1,4-dihydropyridines in protic and aprotic media. *Journal of The Electrochemical Society*, 146(4), pp. 1478-1485.

O'Reilly, J.E. and Elving, P.J., 1971. Electrochemical reduction of pyrimidine in acetonitrile: behavior of the anion free radical. *Journal of America Chemistry Society*, 93(8), pp. 1871-1879.

Pasha, M.A., Swamy, N.R. and Jayashankara, V.P., 2005. One pot synthesis of 3,4-dihydropyrimidin-2(1H)-ones/-thiones catalyzed by zinc chloride: an improve procedure for the Biginelli reaction using microwaves under solvent free condition. *Indian Journal of Chemistry*, 44B(4), pp. 823-826.

Pletcher, D. 2009. *A first course in electrode processes*. 2nd ed. Cambridge: RSC Publishing.

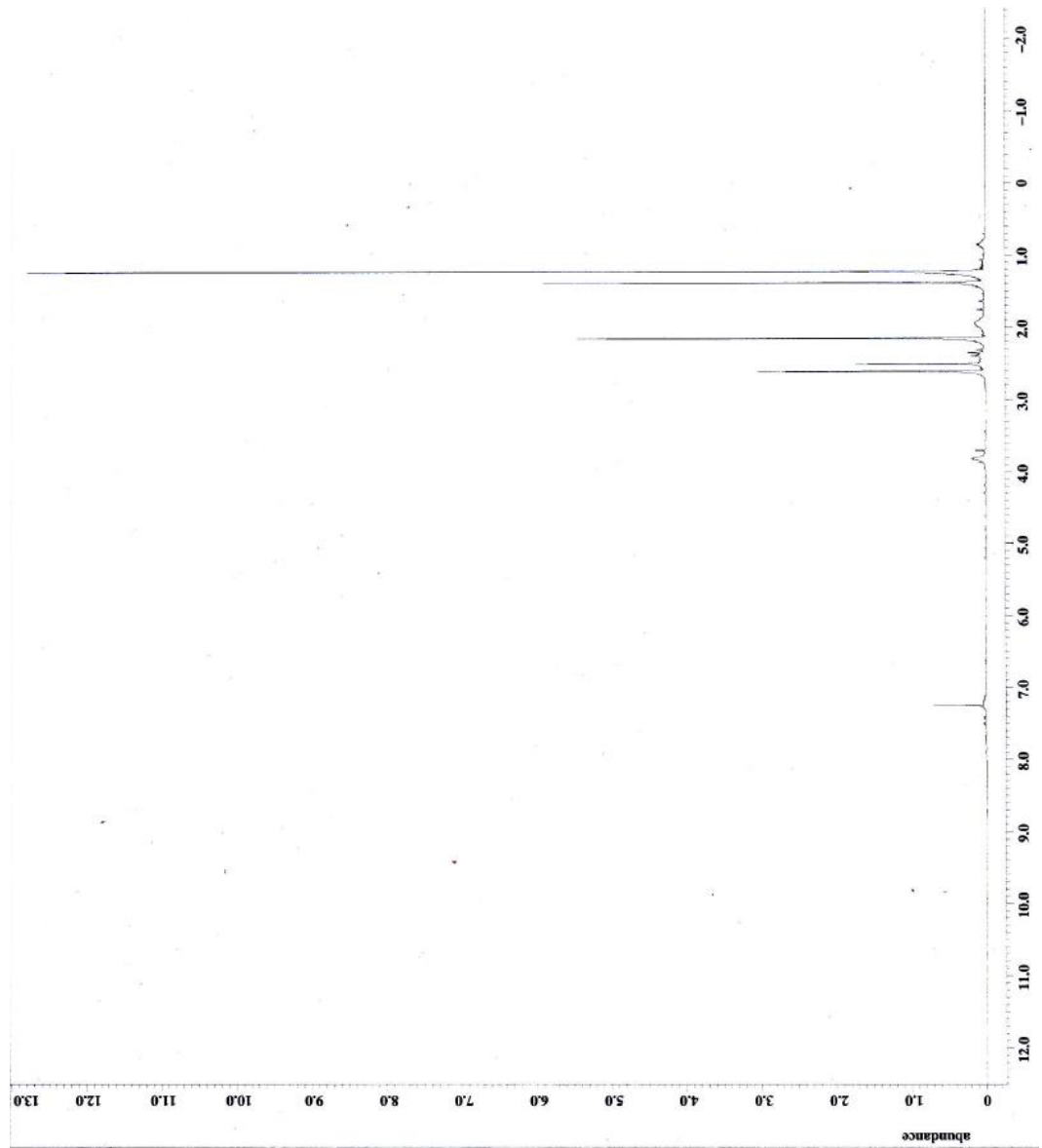
Sperry, J.B. and Wright, D.L., 2006. The application of cathodic reductions and anodic oxidations in the synthesis of complex molecules. *Chemical Society Reviews*, 35(7), pp. 605-621.

Volke, J. and Liška, F., 1994. *Electrochemistry in organic synthesis*. Berlin Heidelberg: Springer-Verlag.

Zanillo, P., 2003. *Inorganic electrochemistry: theory, practice and application*. Cambridge: The Royal Society of Chemistry.

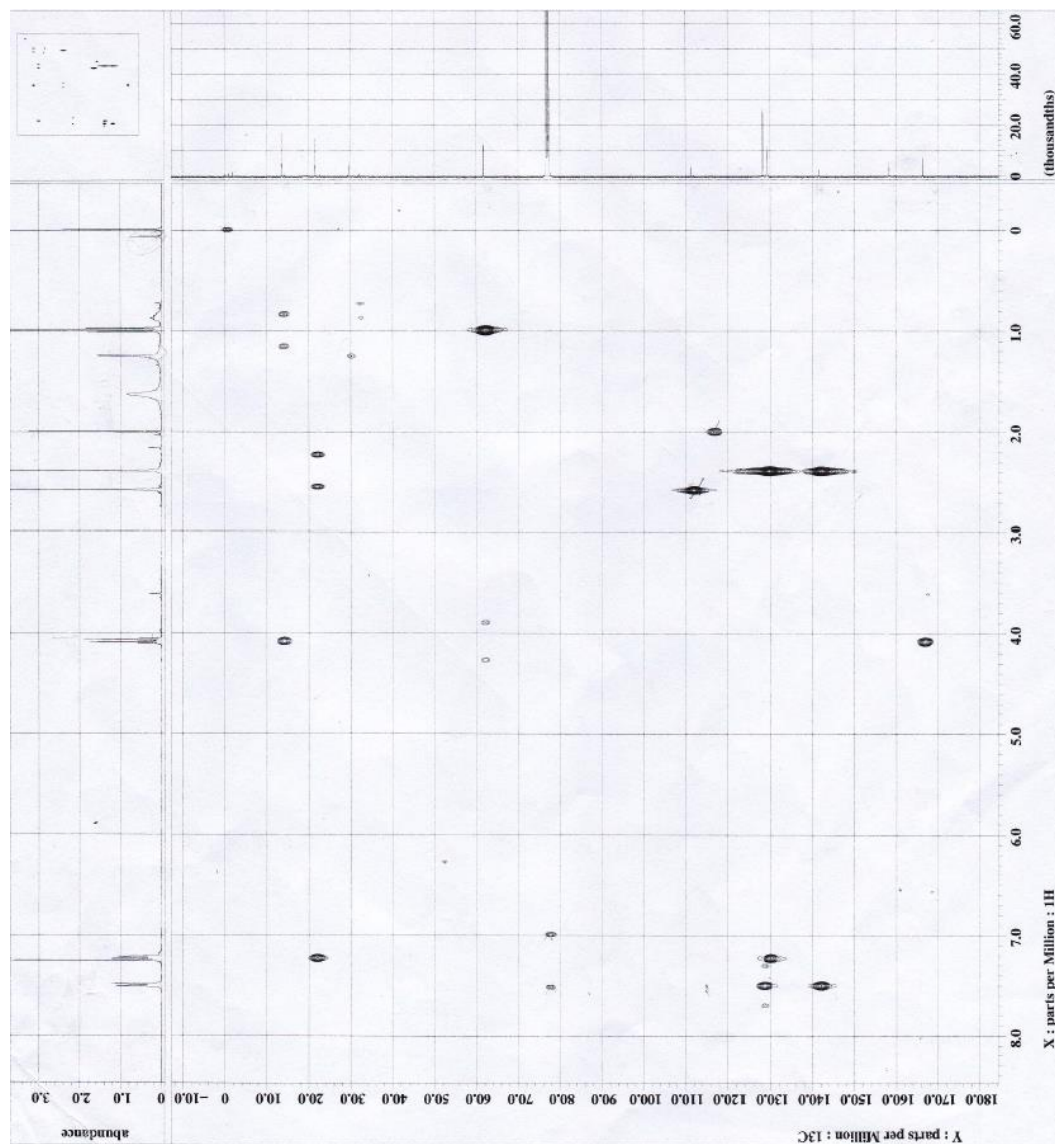
Appendix A

^1H NMR Spectrum of Unwanted Stuff



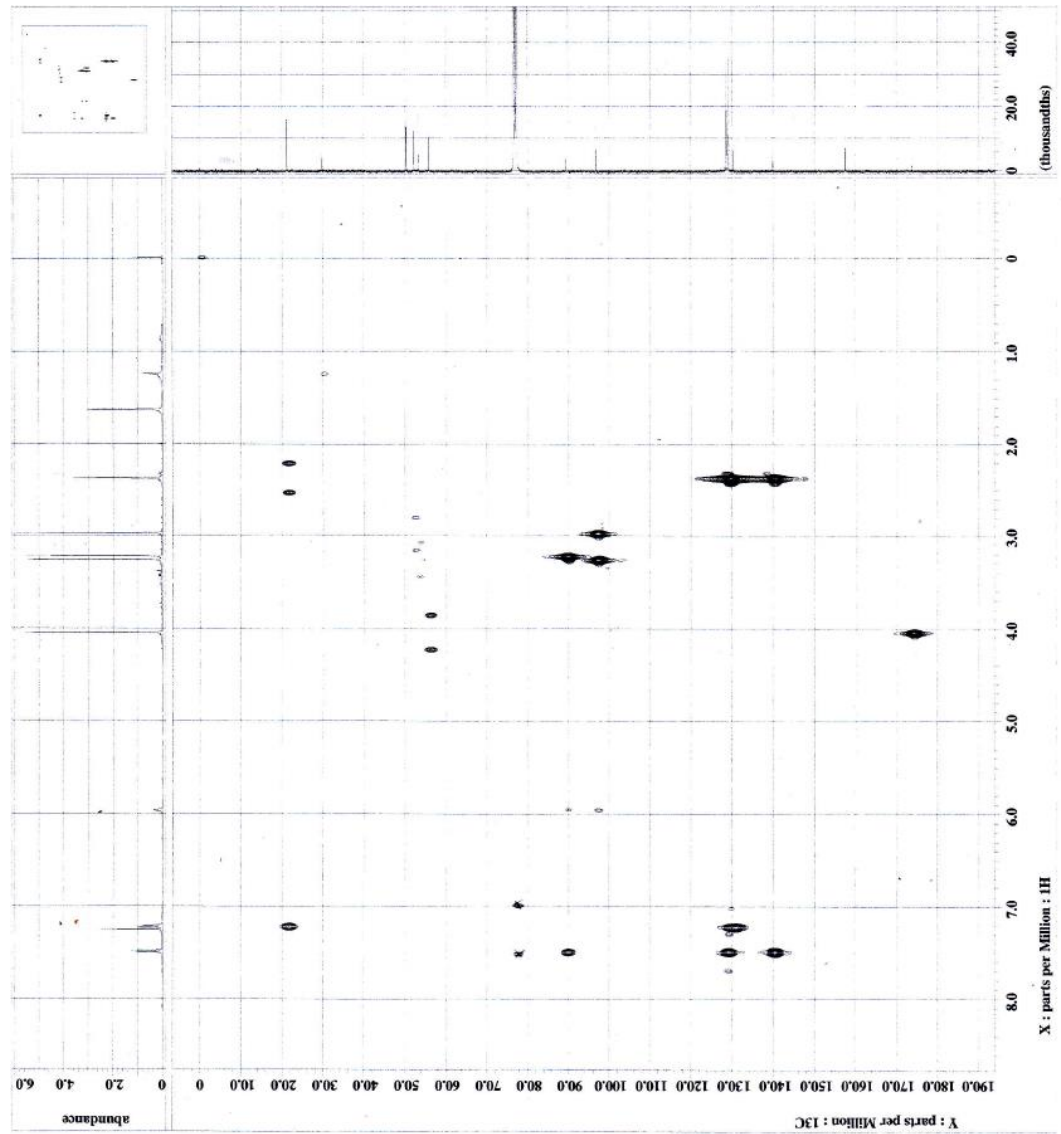
Appendix B

HMBC Spectrum of GWS002



Appendix C

HMBC Spectrum of GWS003



Appendix D

HMBC Spectrum of GWS004

